# Comprehensive Study on Transformer Fault Detection via Frequency Response Analysis

Kakolaki, Seyed Ebrahim Hosseini; Hakimian, Vahid; Sadeh, Javad; Rakhshani, Elyas

**DOI**
10.1109/ACCESS.2023.3300378

**Publication date**
2023

**Document Version**
Final published version

**Published in**
IEEE Access

IEEE Access
Multidisciplinary | Rapid Review | Open Access Journal

Received 28 June 2023, accepted 23 July 2023, date of publication 1 August 2023, date of current version 9 August 2023.

*Digital Object Identifier 10.1109/ACCESS.2023.3300378*

SURVEY

# Comprehensive Study on Transformer Fault Detection via Frequency Response Analysis

**SEYED EBRAHIM HOSSEINI KAKOLAKI[1,*], VAHID HAKIMIAN[1,*], JAVAD SADEH[1], AND ELYAS RAKHSHANI[2], (Senior Member, IEEE)**

[1]Faculty of Engineering, Ferdowsi University of Mashhad, Mashhad 91779, Iran
[2]Department of Electrical Sustainable Energy, Delft University of Technology, 2628 CD Delft, The Netherlands

Corresponding authors: Elyas Rakhshani (rakhshani@ieee.org) and Javad Sadeh (sadeh@um.ac.ir)

*Seyed Ebrahim Hosseini Kakolaki and Vahid Hakimian contributed equally to this work.

**ABSTRACT** The sudden outage of a transformer due to a fault can cause irreparable damage to the electricity industry. Hence, by conducting momentarily inspections of the transformer's condition, faults can be promptly detected, and the transformer can be disconnected from the power grid to prevent subsequent failures in this equipment. Detecting faults at an early stage can also result in reduced repair costs. One recent promising technique for fault detection is Frequency Response Analysis (FRA), which compares the transformer's response in healthy and faulty conditions for understanding the occurrence of transformer faults. This paper presents a comprehensive and accurate modeling approach for the behavior of the transformer at different frequencies, followed by an exposition of the requirements for implementing this method in order to find the fault type, severity, and location. Additionally, various methods for analyzing the results of frequency response are introduced and discussed. In this regard, attempts have been made to introduce advanced complementary methods to address the weaknesses and limitations of the frequency response method. Finally, the concepts are summarized, and suggestions for further research with applications in this field are presented and compared.

**INDEX TERMS** Transformer fault detection, frequency response analysis, hybrid model, ladder model, configuration-transfer function pair, artificial intelligence, online frequency response analysis.

## I. INTRODUCTION

A transformer consists of several components, including windings and cores (known as electrically and magnetically active parts, respectively), bushings, solid and liquid insulators (mainly insulators between high voltage windings and transformer body, an insulator between high voltage and low voltage windings, an insulator between low voltage windings and transformer core) and possibly tap changer. The occurrence of untimely and unexpected failure in any of the mentioned components can occur due to various stresses such as electromagnetic stresses, dielectric stresses, thermal stresses and chemical factors [1].

In general, fault detection methods in power transformers can be divided into three categories: physical, chemical, and electrical methods. Physical methods are based on the measurement of quantities such as the temperature and vibration of a transformer. However, these are the chemical and electrical methods that provide more useful information about the condition of the transformer. Various physical and chemical methods have been studied [2], including the method of assessing the viscosity of insulation, polarization indicator of insulation, as well as the dissolved gas analysis (DGA) method and the optical spectroscopy technique, which are discussed in the references [3], [4], [5]. For the sake of brevity, mentioning other methods has been avoided. Furthermore, various electrical fault detection methods rely on the signals received from the transformer, including methods based on dielectric dissipation factor (DDF), leakage reactance, polarization, and insulation partial discharge (PD) detection. These methods can be classified into basic and advanced categories. One of the advanced electrical methods for fault detection of transformers is the FRA method. This method, due to its non-destructive nature and high sensitivity

The associate editor coordinating the review of this manuscript and approving it for publication was Mehrdad Saif.

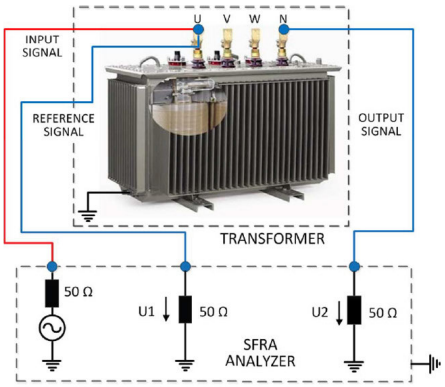


**FIGURE 1.** FRA measurement layout [6].

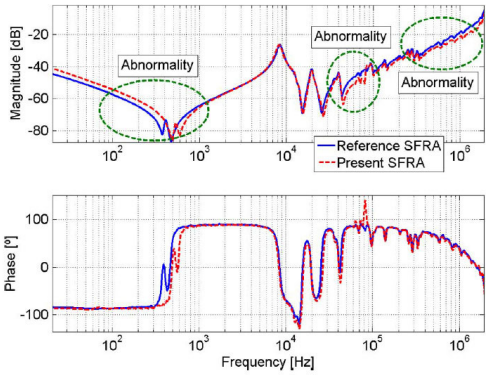


**FIGURE 2.** Power transformer frequency responses comparison [6].

in fault detection, has gained significant popularity among researchers in this field. The subject of this paper focuses on the FRA method.

A transformer can be primarily modeled using three elements: resistor, inductor, and capacitor, each representing various parts of the transformer. As a result, a unique frequency response can be obtained for a healthy and non-defective transformer (which is referred to as a ''signature'' or ''fingerprint''). Consequently, any mechanical or electrical defects, originating from various sources, can alter the transformer's structure, thereby changing the values of its modeling elements and consequently leading to a corresponding change in the frequency response of the equipment. Mechanical failure usually occurs due to improper transport of this equipment, winding deformation due to a short circuit in the power grid and failure of the bushing or transformer core. On the other hand, electrical faults have a variety of causes, such as loss of insulation between the windings and inter-turn short-circuit connections. The process of conducting the FRA test, as seen in FIGURE 1, involved considering the two terminal pairs of the transformer as input-output. Then a signal is applied to the input terminal and the response signal from the output of the transformer is measured for different frequencies. Then the ratio of the output signal to the input is considered the transfer function or the frequency response of the transformer. In FIGURE 2, the magnitude and phase of the transformer frequency response are drawn in two healthy and faulty states. The presence of any abnormality in this diagram indicates the occurrence of a fault in this equipment.

In the following sections, further discussion is provided regarding the characteristics of the applied voltage signal as input, taking into consideration the configuration of the transformer for conducting this test.

In the field of transformer fault detection, the FRA test has emerged as a promising method to identify the type, severity, and location of faults. By comparing the frequency response of a transformer in both healthy and faulty conditions, it is possible to determine the changes that occur in the transformer's behavior due to the presence of a fault.

One of the main advantages of FRA testing is that it enables quick and accurate identification of the type and location of faults. By identifying the faulty component, the duration and cost of repair can be significantly reduced. Additionally, knowledge of the fault severity is also critical in determining the appropriate course of action. For example, if a short-circuit fault occurs multiple times between the winding loops in one part of the transformer, and with considerable severity, it may be necessary to strengthen the insulation of that part to prevent future failures. It is important to note that the ultimate goal of research in this field is to achieve effective and reliable fault detection. By identifying the type, severity, and location of faults, it becomes possible to prevent catastrophic transformer failures that can lead to significant economic and environmental damage. Therefore, all efforts are made with the FRA test to achieve these goals, and researchers are continually seeking new and innovative methods to improve the accuracy and efficiency of transformer fault detection which is the topic that is going to be addressed in this paper. The rest of the paper is consisting of the following sections:

In section II, various methods of modeling transformers at different frequencies are presented to provide a comprehensive understanding of the behavior of this equipment to the readers.

Regarding FRA, transformer modeling holds importance in two ways:

1) As shown in section IV, one of the FRA interpretation methods is based on transformer modeling and comparison of equivalent circuit parameters between the healthy and faulty states.
2) Different faults can be simulated by modeling the transformer and with altering the parameters of the equivalent circuit. Subsequently, the FRA traces obtained from the model can be compared with those recorded from the actual transformer. This enables the identification of fault type, severity, and location, which will be discussed in section IV [7], [8].

In section III, the requirements for implementing the FRA method are discussed. Specifically, the appropriate configuration and transfer function for this task are examined, along

with the proposition of comprehensive criteria for their suitability. In the following, the characteristics and type of input reference signal to be applied to the transformer for FRA will be discussed and the strengths and weaknesses of each of them will be expressed. Then, different solutions to achieve the frequency response of the transformer in a healthy state are presented, and it is shown that even if the transformer frequency response in a healthy state is not available, it is still possible to detect the fault severity. In section IV, first, various methods for analyzing FRA results are introduced and compared. Subsequently, attempts are made to propose different methodologies which can cover the weaknesses of the FRA method. In the following, the effect of winding type, residual flux and other factors affecting FRA are investigated and after fully understanding the behavior of these factors, the problem of determining the appropriate frequency range for the FRA method is expressed. The study demonstrates that various types of faults affect specific regions of the frequency spectrum, and they can also have distinct impacts on the equivalent circuit parameters.

Finally, the FRA online method will be introduced and compared with the offline ones, and the challenges of the online method will be presented. Section V is devoted to summarizing the key findings and presenting recommendations for further research in this field.

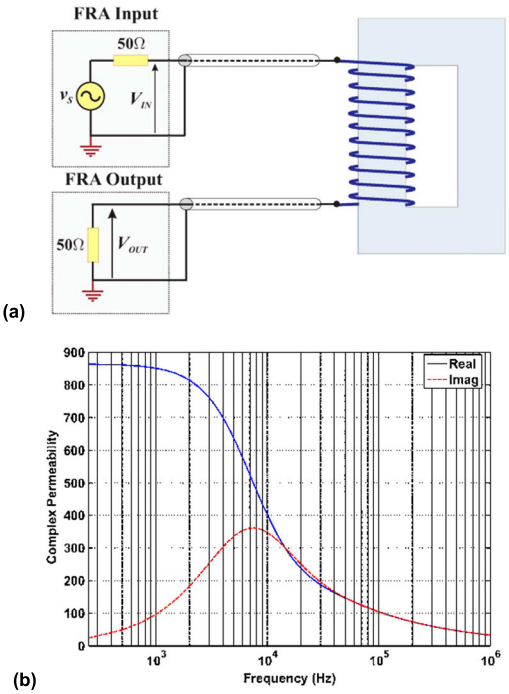


**FIGURE 3.** (a) Schematic of the FRA experiment for a ferromagnetic core. (b) Real and imaginary parts of the magnetic permeability coefficient of the core [3].

## II. TRANSFORMER FREQUENCY MODEL

In FRA, transformer modeling at different frequencies can be used as an approach for fault identification. In this approach, first, the transformer is modeled using an equivalent circuit. After modeling, if there are mechanical or electrical faults, one or more parameters of this model will change and thereby altering the frequency response of this model. Eventually, by comparing and matching the FRA trace obtained from the actual transformer with the one generated from the equivalent circuit, the type and severity of any mechanical fault in the transformer can be identified.

In this section, the behavior of dielectrics and ferromagnetic materials in the presence of time-varying electric and magnetic fields is explained. After describing the behavior of these materials in the presence of time-varying fields, transformer modeling at different frequencies is done.

### A. BEHAVIOR OF FERROMAGNETIC AND DIELECTRIC MATERIALS IN THE PRESENCE OF TIME-VARYING FIELDS

Reference [9] shows that the magnetic permeability coefficient of a material is frequency dependent (see FIGURE 3). The reason for this phenomenon is that magnetic dipoles always tend to be in the direction of the magnetic field. As the frequency increases, since the direction of the field changes rapidly, these dipoles fall behind the applied magnetic field and cannot quickly follow the direction of its change. This lag of the dipoles leads to a delay and manifests itself as a complex number. Therefore, the magnetic permeability coefficient of a material will be a complex number whose real and imaginary parts depend on frequency. The same behavior occurs for a dielectric in the presence of a time-varying electric field, which means that the electrical conductivity of these materials is a complex number and its real and imaginary parts will be frequency dependent [10]. Reference [10] shows that the resistance, capacitance and inductance values of the transformer model are dependent on the frequency, and this issue complicates the modeling of the transformer for the purpose of FRA and fault detection. Nevertheless, it is possible to consider the values of these parameters constant and independent of frequency by accepting a small amount of reduction in modeling accuracy.

### B. TRANSFORMER MODELING

#### 1) HYBRID MODEL OF TRANSFORMER

According to [11], based on the theory of the long transmission line (in which the line parameters are distributed along the line and at small distances $\Delta x$), a coil has been modeled which itself consists of several disks and each disk consists of several loops (shown in FIGURE 4). As each disk in this method is modeled based on the theory of traveling waves and the equivalent circuits of the disks are connected to each other, the method is referred to as the hybrid method. In fact, in this method, the winding of each phase is considered as several transmission lines (each disk, one transmission line) and each transmission line is modeled as a long transmission line based on the theory of traveling waves. The parameters related to the mentioned model can be extracted through analytical relations (formulas) or to achieve higher accuracy through the finite element method (FEM) [10], [12], [13], [14]. The

mentioned hybrid model is very complex and it is possible to present another model with a slight reduction in its accuracy, named the ladder model [15]. On the other hand, due to the simplifying assumptions that exist in analytical relationships to determine the parameters of a hybrid model, the accuracy of modeling is reduced. Also, parameterization can be determined through analytical relationships, but this requires access to information about the transformer's structure and geometry, which is not usually the case. Because transformer manufacturers do not provide this information to users. Incorporation of different optimization techniques can be considered as an alternative approach for solving the recent problem.

#### 2) TRANSFORMER LADDER MODEL AND METHODS OF DETERMINING ITS PARAMETERS

Reference [15] presents the transformer ladder model. The idea is that in the hybrid method, each disk is considered as a long transmission line and normally should be modeled using distributed parameter model, but by accepting a slight reduction in modeling accuracy, in this case, each or more disks are modeled as a lumped model. FIGURE 5 shows the ladder model of phase X of a three-phase transformer. Again, the values of the parameters are calculated through analytical relations [16]. By considering the capacitors' voltage and inductor current as state variables in the ladder model, different transfer functions can be defined. Using meta-heuristic optimization algorithms, the parameter values of the ladder model are extracted. In this reference, the objective function of the optimization problem is considered as a weighted sum of the differences between the three defined transfer functions and their measured values. By minimizing the mentioned objective function, the equivalent circuit parameters of the ladder model are derived. As previously mentioned, the model parameters can be extracted through simulation in FEM software. However, this method is only possible if complete information regarding the transformer's structure is available. In [17], after using analytical formulas as the initial conditions for the bacterial swarming optimization algorithm (BSA), it has been concluded that the parameters obtained from the optimization with BSA had more accurate performance in transformer modeling in comparison with the analytical formulas.

Therefore, it is concluded that in the ladder model, it would be very desirable if the FEM could be used to find its parameters. But if only analytical relations are available, it is better to use them as the initial conditions for the BSA to achieve the parameters more accurately. In addition, the study used a genetic algorithm (GA) along with BSA. The results showed that the parameters obtained through BSA were the most successful in accurately modeling the transformer, followed by those obtained through GA and analytical relations, in descending order. It is worth noting that in order to reduce the computational burden in the optimization problem, the matching between the ladder model transfer function and the measured one is not performed for the entire frequency range and only the important points of the frequency response, i.e. the points corresponding to the resonance frequencies (peaks of the transfer function) and anti-resonance frequencies (troughs of the transfer function), are considered.

The reference [18] also uses a GA to adapt the frequency response of the ladder model with the frequency response obtained from the measurement. But this adaptation is not like the reference [17] that is done only for the resonance and anti-resonance frequencies, nor is it like the other references related to the transformer ladder modeling that is done for the whole frequency range of the adaptation, but between the two. That is, it is done for a series of frequencies that include resonance and anti-resonance frequencies. The reference [19] using the artificial bee colony (ABC) optimization algorithm, deals with the problem of constructing a ladder model based on driving-point impedance (DPI) as a network transfer function in a similar way to the reference [17]. The created model has acceptable accuracy. In reference [20], the determination of ladder model parameters was compared using analytical relations, particle swarm optimization (PSO) algorithm, and improved particle swarm optimization (IPSO) algorithm. The results showed that the parameters optimized with the IPSO algorithm were better than those obtained with the PSO algorithm. Moreover, the PSO algorithm was found to contribute to more accurate modeling of transformers compared to using analytical relations. Reference [21] also deals with determining the parameters of the transformer ladder model using two optimization algorithms, GA and PSO, and the results show that this approach can accurately estimate the parameters of the transformer ladder model in both healthy and fault states.

So, the frequency response resulting from the simulation of the model follows the measured frequency response very accurately.

In reference [22], the authors attempt to determine the parameters of the ladder equivalent circuit using GA and emphasize that in practice, the transformer winding structure is not homogeneous and therefore, the assumption of equality of the parameters of the ladder model sections, reduces the modeling accuracy. Therefore, it is better to consider the parameters of each section as a separate variable in the optimization problem. Also, if the optimization problem is solved unconditionally, it may provide answers that are practically impossible. For example, it is clear that the mutual inductance between the first and second sections must be greater than the mutual inductance between the first and third sections of the ladder model. Thus, in this reference, firstly, an optimization problem with inequality constraints is solved. Secondly, two different case studies, namely homogeneous and non-homogeneous models for transformer windings, are considered. Finally, it has been concluded that in practice, the parameters of different sections in the ladder model should be treated as different and distinct variables in order to improve the accuracy of the model (non-homogeneous winding). But in [23], the transformer is modeled by considering

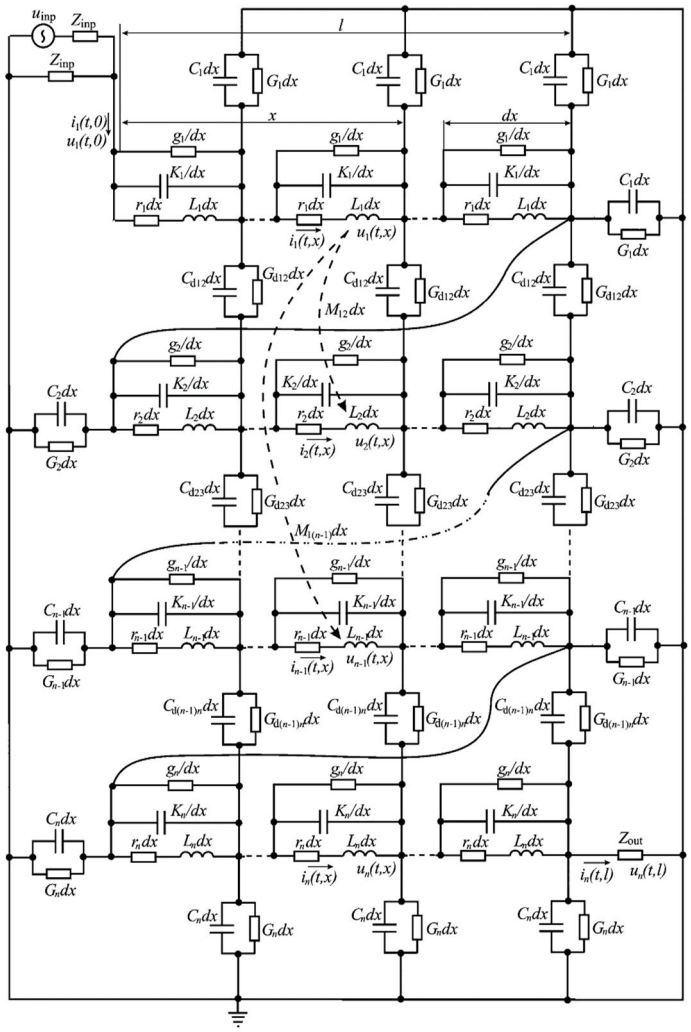


**FIGURE 4.** Transformer hybrid model with disk winding [11].

both equivalent circuits, i.e. the hybrid model and the ladder model, and determining their parameters through analytical relations as well as the GA, and show that as expected, the results of the hybrid model is closer to the measured actual value and also the parameters of both optimization models are closer to the actual measured values than the parameters obtained through analytical relations. It is worth mentioning that the series capacitor value can be calculated through FEM or analytical relations. However, this requires information about the structure and geometry of the coil. While using the optimization algorithms, the values of the parameters of the ladder model, including the series capacitor, can be obtained.

Reference [24] presents another method based on the estimation of the transfer function from the measured frequency response, in order to extract the parameters of the ladder model, including the series capacitor. This reference by measuring the earth capacitance, estimates the series capacitor. The process of determining the value of the series capacitor is shown in FIGURE 6. First, the impedance of the excitation point of the transformer is measured and its amplitude and phase are obtained. Then, using the method presented in [25], the best transfer function is adapted to the zero-pole-gain format (equation (1)), where $\tau$ is real zero, $z_i$ and $p_i$ are zeroes and poles of the transfer function, respectively, which appear as complex conjugates. While the value of the gain $\frac{a_0}{b_0}$ is equal to $\lim_{s\to\infty} sZ(s)$ [24].

$$Z(s) = \left(\frac{a_0}{b_0}\right) \frac{(s-\tau)\prod_{i=1}^{n-1}(s-z_i)\left(s-z_i^*\right)}{\prod_{i=1}^{n}(s-p_i)\left(s-p_i^*\right)} \qquad (1)$$

On the other hand, the ladder model with $n$ sections, where $n$ is equal to the number of natural frequencies of the excitation point impedance, is considered for the winding. For high frequencies ($s \to \infty$), only the capacitors of the equivalent circuit are effective, and therefore, the impedance $Z(s)$ (including $C_g$ and $C_s$) is extracted from the ladder model. By multiplying $Z(s)$ by $s$ and setting it equal to $\frac{a_0}{b_0}$, an equation is derived in terms of $C_g$ and $C_s$.

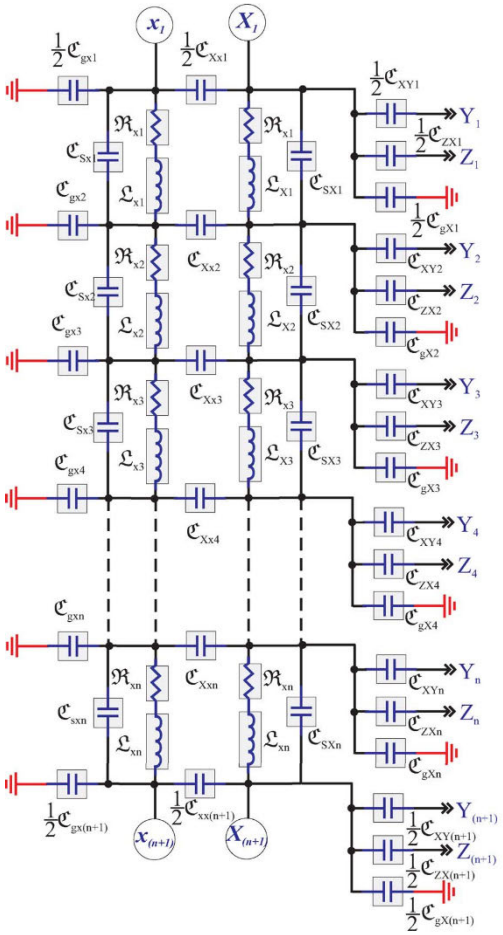

**FIGURE 5.** The ladder model of phase X of a three-phase transformer [9].

By measuring the value of $C_g$, the series capacitor $C_s$ is calculated. Finally, the values of inductance and resistance of the ladder model can also be measured from equation (2) and for low frequencies ($s \to 0$) [25].

$$\lim_{s\to 0} Z(s) = R_{dc} + sL_{eq} \tag{2}$$

By measuring the equivalent inductance $L_{eq}$ and through a repetition-based algorithm, the self and mutual inductance values of different parts of the ladder model are extracted. The resistance of each section of the ladder model is also obtained by dividing $R_{dc}$ by the total number of sections. Another point that should be mentioned is that the number of parts of the ladder model is equal to the number of natural frequencies seen in the impedance of the excitation point. However, not all natural frequencies are visible in the frequency response diagram due to factors such as high damping at high frequencies resulting from the skin effect. To address this issue, a repetition-based algorithm is used to calculate the number of natural frequencies in the excitation point impedance, as well as the appropriate number of sections for the ladder model [26].

It is worth noting that the unknown values of the transfer function (gain, zeroes and poles) can be obtained in various ways, such as the vector fitting (VF) method, which operates on the basis of the least squares estimation (LSE) method [27]. The basis of the VF method is that it adapts the best transfer function of degree $n$ which is equal to the number of measured impedance poles, to the transfer function calculated by an iterative method. By the way, this algorithm is sensitive to its initial conditions, i.e., the initial values of the poles and also, the number of iterations and, more importantly, the degree of the estimated transfer function. The reference [28] provides a solution to improve this algorithm.

As explained before, the hybrid and ladder models both describe the transformer's behavior over the entire frequency range. However, as shown in the next sections, to detect faults and their locations, modeling the transformer at low and medium frequencies is necessary.

### 3) LOW AND MEDIUM FREQUENCY MODEL OF TRANSFORMER

In this section, two different transformer models with two approaches are presented in low (lower than 2 kHz) and medium (between 2 kHz and 20 kHz) frequencies.

#### *a: DUALITY-BASED LUMPED EQUIVALENT CIRCUIT OF THE TRANSFORMER*

In [29], [30], [31], [32], [33], [34], [35], and [36], the modeling of the transformer in low and medium frequencies is discussed, which is based on the development of the transformer reluctance model. The modeling process is presented as follows.

Considering the paths of flux in the transformer, at first, its reluctance model is extracted (FIGURE 7-a and FIGURE 7-b). Then, based on the duality principle, each reluctance is replaced by an inductance, voltage source by current source and node by mesh (FIGURE 7-c and FIGURE 7-d). On the other hand, due to the ratio of turns of transformer coils, any current source becomes an ideal transformer. Finally, by adding the resistors that model transformer losses and the capacitors between each of the high-voltage and low-voltage coils as a lumped element along with ground capacitors, the final model for a three-phase transformer is derived (FIGURE 8). The values of inductances and the resistances of the equivalent circuit can be extracted through three tests including short-circuit, open circuit and zero sequence tests.

In terms of measurement, the capacitors of this model are divided into two categories: measurable and non-measurable. Measurable capacitors include ground capacitors and capacitors between high and low voltage windings, and non-measurable ones include series capacitors and capacitors between high voltage windings as well as capacitors between low voltage windings.

The values of measurable capacitors are extracted through a capacitive impedance test. The value of the series capacitor

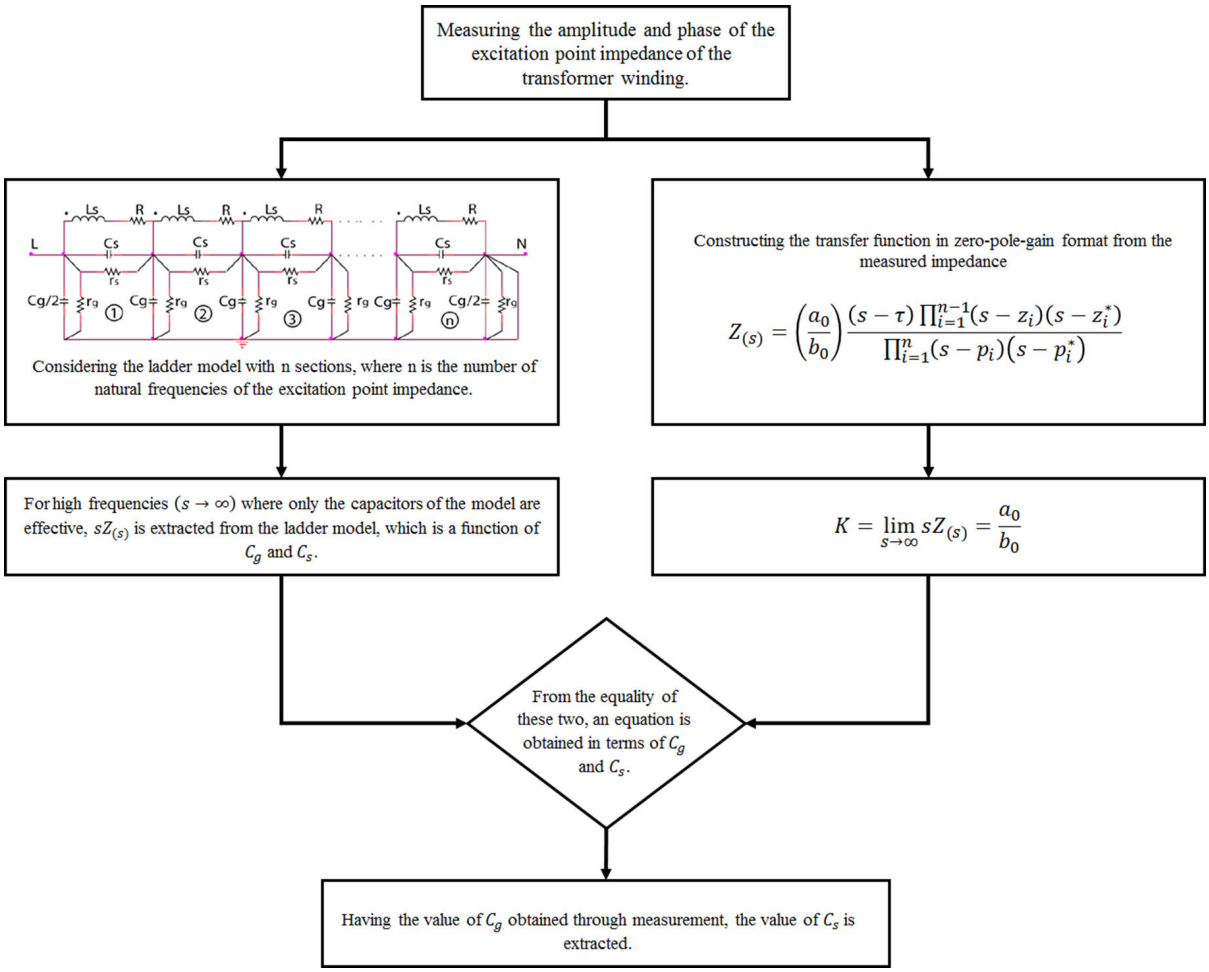


**FIGURE 6.** The process of estimating the value of the series capacitor of the transformer winding ladder model based on the impedance of the excitation point.

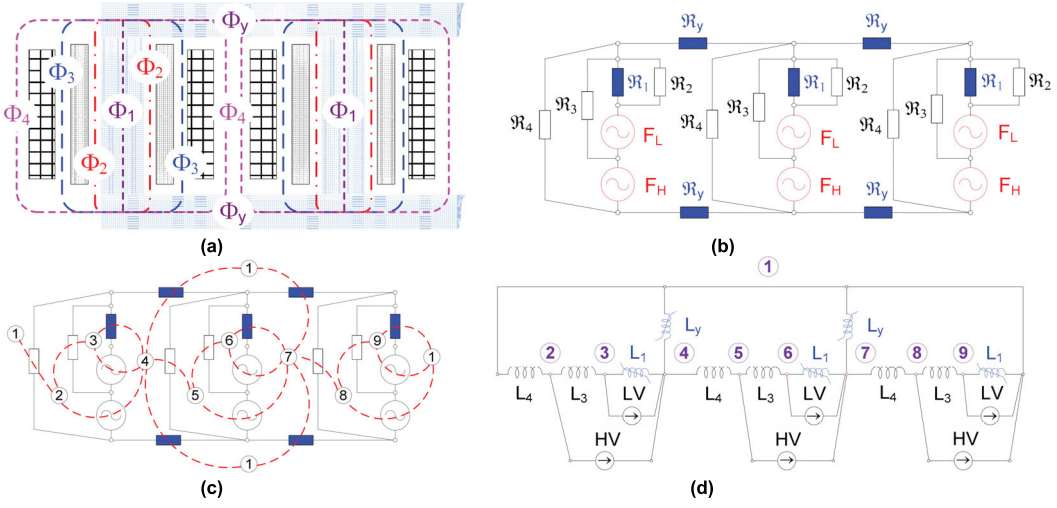


**FIGURE 7.** Model extraction procedure of duality based lumped equivalent circuit of transformer [33].

cannot be measured directly and, therefore, an estimated value is used. It is possible to estimate the capacity of the series capacitor with high accuracy with the approach mentioned in the previous section [24]. Therefore, the values of the parameters of the duality based lumped model are calculated by measuring the impedance of the excitation

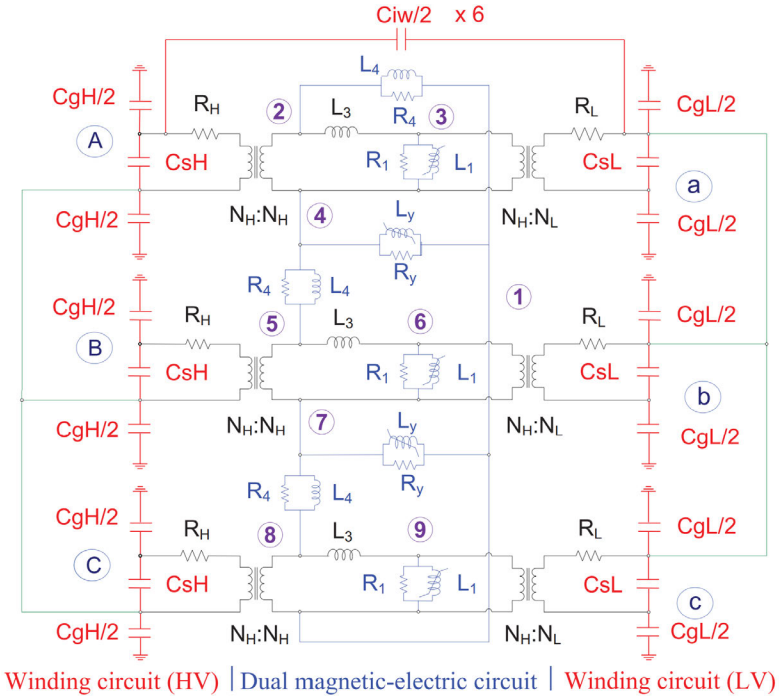


**FIGURE 8.** Lumped duality based equivalent of an Yy6 transformer [33].

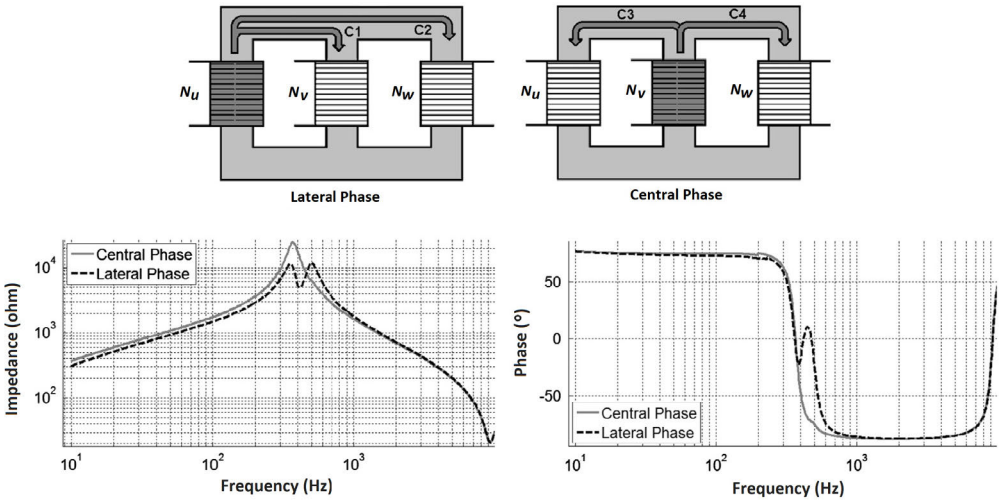


**FIGURE 9.** (a) Flux flow paths in three-phase transformer. (b) Amplitude and phase of input impedance measured in different phases [37].

point [29], [30], [31], [32], [33]. Since the parameters of duality-based lumped model are calculated based on different input impedances, this approach is known as the impedance method [32]. Also, the values of the parameters of the duality based lumped model can be calculated through the analytical relationships and the information provided by the transformer manufacturers (manufacturer data sheet) [33], [34], [36].

Reference [35] uses the zero-crossing method based on waveform data to determine the parameters of the duality based lumped model. In [33], a comparison is made between the low frequency model of the transformer and the hybrid model and the results show that both duality based lumped model and hybrid models can be used for FRA analysis in low and medium frequencies with very good accuracy [31]. But in high frequencies, the hybrid model is more suitable for analysis. In some medium and high frequencies, the duality based lumped model does not have enough accuracy, which is also confirmed by reference [30].

Based on [32], it is suggested to use the duality based lumped model for the analysis in low and medium

frequencies, because its parameters are easily determined through measurement. But for the analysis in high frequencies, the hybrid and ladder models are used for their high accuracy.

Also, the values of the capacitors of different segments of the hybrid model can be easily found from the values of their corresponding capacitors in the duality based lumped model, taking into account the number of segments and without the need to use analytical relations. This can be seen as an advantage, because analytical relationships require complete information about the structure of the transformer [36].

### b: MULTI-CELL EQUIVALENT CIRCUIT OF THE TRANSFORMER

In [37], taking into account the simplifying assumptions in the transformer reluctance model described in previous sub-section, using the impedance measured in each phase of the transformer and with an optimization approach, the parameters of the model at low and medium frequencies are determined. The process of modeling and determining its parameters is presented as follows.

First, the input impedance of the different phases of the transformer is measured (FIGURE 9).

As it can be seen in FIGURE 9, two common features in all three-limb core-type transformers can be pointed:

1) The length of the magnetic path of the middle phase is less than the length of the magnetic path of the lateral phases.
2) The magnetic path of the lateral phases is equal to each other due to the existing symmetry, and for this reason, the reluctance of the lateral phases are equal to each other.

This factor causes the measured frequency response curve of lateral and middle phases to be different. Therefore, two resonance peaks are created in the frequency response of lateral phases due to asymmetric magnetic paths C1 and C2 in FIGURE 9. Meanwhile, a resonance peak is created in the frequency response of the central phase due to the symmetrical magnetic paths C3 and C4.

3) After measuring the input impedance of different phases, considering the flux paths, the reluctance model of the transformer is extracted (FIGURE 10-a). Based on the duality principle and by adding capacitor and resistor, which respectively model the capacitive effects of windings and transformer losses, the equivalent circuit of FIGURE 10-b is obtained. The elements of each phase, in general, can be shown with an impedance (FIGURE 10-c). By comparing the reluctance model of FIGURE 10-a with the reluctance model of section II-B3.a, it can be seen that the complexity of the model presented in the previous section has been reduced. Now the problem is how by measuring the observed impedances of each phase of the transformer which are denoted by Z_mU, Z_mV and Z_mW respectively, the impedances of each phase of the model, i.e. Z_U (including R_U, L_U and C_U), Z_V (including R_V, L_V and C_V) and Z_W (including R_W, L_W and C_W) are extracted.

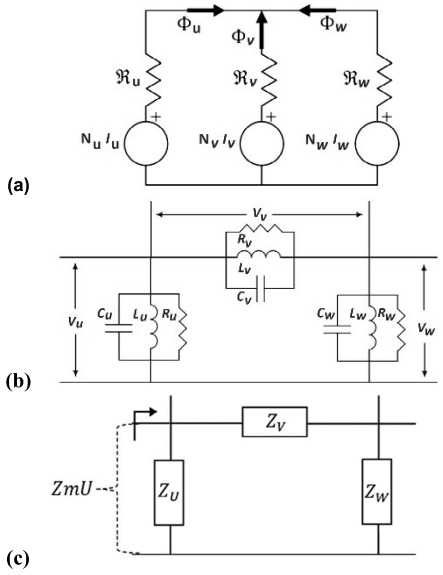


**FIGURE 10.** (a) Transformer magnetic circuit. (b) Transformer core model. (c) Transformer core model represented by three impedances $Z_U$, $Z_V$ and $Z_W$ [37].

According to FIGURE 10-c, each of the measured impedances $Z_{mU}$, $Z_{mV}$ and $Z_{mW}$ can be expressed through three equations, in terms of the impedances of each phase of the model, i.e. $Z_U$, $Z_V$ and $Z_W$ (equation (3)) [37].

$$\begin{cases} Z_{mU} = Z_U \parallel (Z_V + Z_W) \\ Z_{mV} = Z_V \parallel (Z_W + Z_U) \\ Z_{mW} = Z_W \parallel (Z_U + Z_V) \end{cases} \tag{3}$$

In this case, by ordering these three equations, it is possible to obtain the impedances $Z_U$, $Z_V$ and $Z_W$ and of course, their corresponding admittances in terms of $Z_{mU}$, $Z_{mV}$ and $Z_{mW}$. Finally, the values of the elements of each phase of the presented model are obtained by minimizing the following objective function for each phase (here phase U) and for $m$ samples of the frequency response (here $Z_U$) [37].

$$E = \sum_{i=1}^{m} \frac{\left| Y_U(\omega_i) - \frac{1}{R_U} - j.\left(C_U\omega_i - \frac{1}{L_U\omega_i}\right)\right|^2}{|Y_U(\omega_i)|^2} \tag{4}$$

Comparing the results of the model simulation with the measured values indicates that the proposed model can accurately capture the transformer behavior in low and medium frequencies.

References [38] and [39] also use the impedance measured in each phase of the transformer. Also, their method is based on the multi-cell equivalent circuit, which each cell is equivalent to a parallel R-L-C circuit. As a result, for each phase of the transformer shown in FIGURE 11, the values of the model elements in FIGURE 10-b are extracted.

A parallel connected R-L-C circuit has one resonance frequency. Therefore, a two-cell equivalent circuit is considered

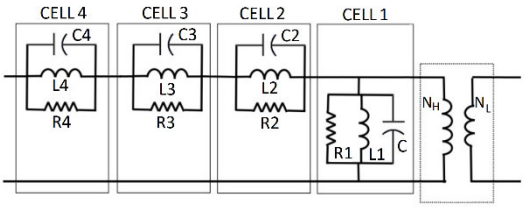


**FIGURE 11.** Four-cell equivalent model [38].

for the lateral phases and a single-cell equivalent circuit is considered for the middle phase.

Having the input impedance of each phase obtained through measurement, the values of the elements of each cell are calculated through the minimization of the objective function, similar to equation (4). Finally, the values of the elements of the model in FIGURE 10-b can be easily extracted from the values of the multi-cell equivalent circuit elements through mathematical relationships.

## III. FRA REQUIREMENTS

In this section, a comprehensive review on the requirement of implementation of the FRA method is presented and analyzed. In this war, various topics such as selecting the appropriate configuration and transfer function pair to analyze the frequency response, selecting the appropriate voltage range for the FRA method, types of reference signals that can be used for the FRA method is discussed and compared. Furthermore, different methodologies to achieve the transformer frequency response in a healthy state with a review over the possibility of detecting the fault severity especially when the transformer frequency response is not available in the healthy state, are presented and discussed.

### A. SELECTION OF THE APPROPRIATE CONFIGURATION AND TRANSFER FUNCTION PAIR

Regarding FRA, it is important to note that a transformer has multiple terminals, and the conditions of these terminals can vary depending on whether they are grounded or open. The main problem is to find the best configuration and, consequently, the appropriate transfer function to perform the FRA test. Each configuration is equivalent to a new network with a number of natural frequencies. Due to the possible cancelation of zeroes and poles, all or part of the natural frequencies of such a network appear in the different transfer functions. In order to increase the sensitivity and fault detection capability of the FRA test, it is necessary that all or most of the natural frequencies of the network are available. Therefore, as shown in FIGURE 12, it is essential to determine the best configuration and transfer function pair to achieve this goal. For this purpose, reference [40] investigates different types of configuration and transfer function pairs (FIGURE 12) according to the number of natural frequencies that appear in them and divides them into four categories: good, reasonable, medium and bad (TABLE 1). Another important point is that, among those configuration and transfer function pairs suitable for FRA test, some of them have more sensitivity for a specific fault and are more suitable for detecting that type of fault. Therefore, it is possible to choose the appropriate configuration and transfer function pair for a specific fault to perform the FRA test [41].

Reference [42] deals with which configuration with the specified transfer function is more sensitive to the occurrence of three types of AD, RD and axial bending (AB). To achieve this goal, five different configurations with three transfer functions are considered. The procedure used in this reference to determine the best configuration and transfer function pair is such that various faults are applied and by observing the frequency response changes, it is investigated which configuration and transfer function pair has the highest sensitivity for the specified fault. The results show that for AD and RD faults, transfer voltage ratio configuration and for AB fault, end-to-end voltage ratio configuration have more sensitivity and are more suitable. It is worth mentioning that the two configurations of transfer voltage ratio and end-to-end voltage, being in the good category, have also been approved by reference [40]. Reference [7] follows the same procedure for the AD, RD and disc space variation (DSV) faults, but to select the best one, it resorts to numerical indices rather than visual comparison, because the interpretation of the results by numerical indices is more accurate and logical than the interpretation based on observation. The results indicate that bfloat-oc and pfsg-oc configurations, which are placed in the good and reasonable category in [40], have the best performance for identifying mechanical faults.

According to the standards available to researchers and craftsmen so far, four configurations are usually recommended as shown in FIGURE 13 by selecting the transfer voltage as the transfer function [43], [44]: end-to-end open circuit (EEOC), end-to-end short circuit (EESC), capacitive inter-winding (CIW), and inductive inter-winding (IIW) configuration.

It is worth noting that although there are not many standards and technical reports available on the topic of FRA, some references are particularly valuable. For example, a technical report published by CIGRE focuses on the interpretation and procedure of performing FRA tests [45]. A similar guideline has been presented by IEEE with a focus on oil-immersed transformers [46]. Chinese National Development and Reform Commission (NDRC) has issued a standard about the primitive requirements in FRA on transformer winding deformation [47]. IEC has also published a standard in association with the measurement techniques and equipment in FRA [44]. Finally, one of the most recent practical guidelines about FRA is presented in reference [48] which discusses the measurement fundamentals and methods of result interpretation in FRA.

### B. DIFFERENT METHODS FOR PERFORMING FRA TEST

Another issue is the determination of the type of reference signal for performing the FRA test, which consists of two types [49], [50]:

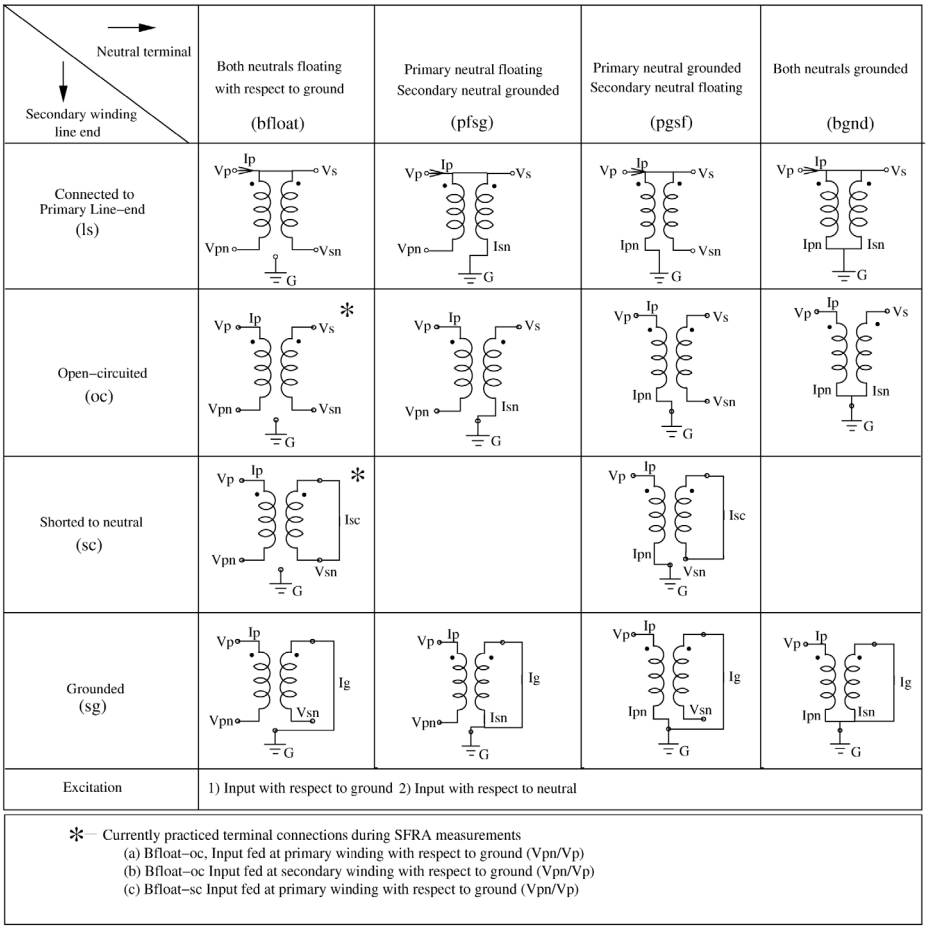


**FIGURE 12.** Various configurations along with measurable quantities [40].

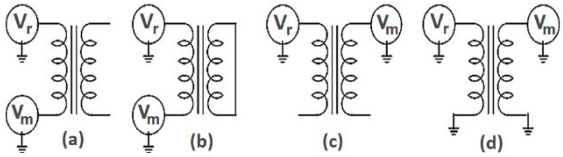


**FIGURE 13.** Different FRA configurations: a) EEOC b) EESC c) CIW d) IIW [43].

1) Impulse frequency response analysis (IFRA) method: In this case, a wide range of frequencies is injected into the transformer by a low voltage impulse signal, in order to perform FRA. Then, the output signal is measured and after passing through the filter to eliminate noise, using the short time Fourier transform, it is transferred to the frequency domain and thus, the transformer frequency response is extracted.
2) Sweep frequency response analysis (SFRA) method: In this method, a sinusoidal signal with a low amplitude from low frequencies to high frequencies is swept and its output is measured. In this case, the output-to-input ratio is considered as a transfer function.

The advantages and disadvantages of the two mentioned methods can be examined from different aspects.

The SFRA method requires less measurement equipment than the IFRA method (oscilloscope, Rogowski coil, and other equipment). SFRA method has a higher signal-to-noise ratio compared to the IFRA method. Also, in the SFRA method, the response exists in the frequency domain in the form of amplitude and phase. But in the IFRA method, it is in the time domain and therefore, there is a need to convert the short time Fourier transform in order to transfer it to the frequency domain. Besides, the resolution is adjustable in the SFRA method, but in the IFRA method, the resolution is fixed. In relation to the subject of adjustable resolution in the SFRA method, it's important to note that various standards require a minimum resolution of at least 200 points per decade or higher in order to accurately detect resonance frequencies. [51]. In the IFRA method, it is possible to measure several outputs, and therefore, several transfer functions can be defined. However, in the SFRA method, only one output can be measured at any time. Testing by IFRA takes less time compared to SFRA which may take up to 10 minutes.

**TABLE 1. Classification of different network function-configuration pairs based on the highest number of natural frequencies in order to determine the best network function-configuration to perform FRA test [40].**

| Excitation | Terminal connection | System function | Expected number of peaks | $\alpha_{primary} : \alpha_{secondary}$ 3 : 3 actual | 4 : 4 actual | 5 : 5 actual | 6 : 6 actual | 7 : 7 actual | 8 : 8 actual | 9 : 9 actual | Remarks |
|---|---|---|---|---|---|---|---|---|---|---|---|
| Input with respect to ground | bfloat-sg | $I_g(\omega)/V_p(\omega)$ | 8 | 7 | 7 | 7 | 7 | 7 | 7 | 7 | Good |
| | bfloat-oc* (i/p to Pri) | $V_{pn}(\omega)/V_p(\omega)$ | 9 | 7 | 7 | 7 | 7 | 7 | 7 | 7 | |
| | bfloat-oc* (i/p to Sec) | $V_{pn}(\omega)/V_p(\omega)$ | 9 | 5 | 6 | 6 | 6 | 6 | 6 | 6 | Reasonable |
| | bfloat-sc* | $V_{pn}(\omega)/V_p(\omega)$ | 8 | 5 | 5 | 6 | 6 | 6 | 6 | 6 | |
| | pfsg-sg | $I_{sn}(\omega)/V_p(\omega)$ | 7 | 5 | 6 | 6 | 6 | 6 | 6 | 6 | |
| | bgnd-oc | $I_{sn}(\omega)/V_p(\omega)$ | 7 | 5 | 5 | 6 | 6 | 6 | 6 | 6 | |
| | pfsg-oc | $I_{sn}(\omega)/V_p(\omega)$ | 8 | 5 | 5 | 6 | 6 | 7 | 7 | 7 | |
| | pgsf-oc | $V_{sn}(\omega)/V_p(\omega)$ | 8 | 5 | 5 | 6 | 6 | 7 | 7 | 7 | |
| | pgsf-oc | $V_s(\omega)/V_p(\omega)$ | 8 | 5 | 6 | 6 | 6 | 6 | 6 | 7 | |
| | bfloat-oc | $V_s(\omega)/V_p(\omega)$ | 9 | 6 | 6 | 7 | 7 | 7 | 7 | 7 | |
| Input with respect to neutral | bfloat-sc | $V_{sn}(\omega)/V_p(\omega)$ | 8 | 5 | 6 | 5 | 6 | 5 | 5 | 5 | |
| Input with respect to ground | bfloat-sg | $V_{pn}(\omega)/V_p(\omega)$ | 8 | 4 | 4 | 4 | 4 | 4 | 4 | 4 | Medium |
| | pfsg-sg | $V_p(\omega)/I_p(\omega)$ | 7 | 4 | 4 | 4 | 4 | 4 | 4 | 4 | |
| | pgsf-sg | $V_{sn}(\omega)/V_p(\omega)$ | 7 | 4 | 4 | 5 | 5 | 5 | 4 | 4 | |
| | pgsf-sg | $I_{pn}(\omega)/V_p(\omega)$ | 7 | 4 | 4 | 4 | 4 | 4 | 4 | 4 | |
| | pfsg-ls | $I_{ls}(\omega)/V_p(\omega)$ | 8 | 3 | 3 | 3 | 3 | 3 | 3 | 3 | |
| | bgnd-ls | $V_p(\omega)/I_p(\omega)$ | 8 | 3 | 3 | 2 | 3 | 3 | 3 | 3 | |
| | bfloat-sc | $V_{pn}(\omega)/V_p(\omega)$ | 8 | 2 | 2 | 2 | 2 | 2 | 2 | 2 | Bad |

*—Currently practiced terminal connections during SFRA measurements (with 50 Ω termination)
—All the remaining data pertain to measurements made with 1 MΩ termination

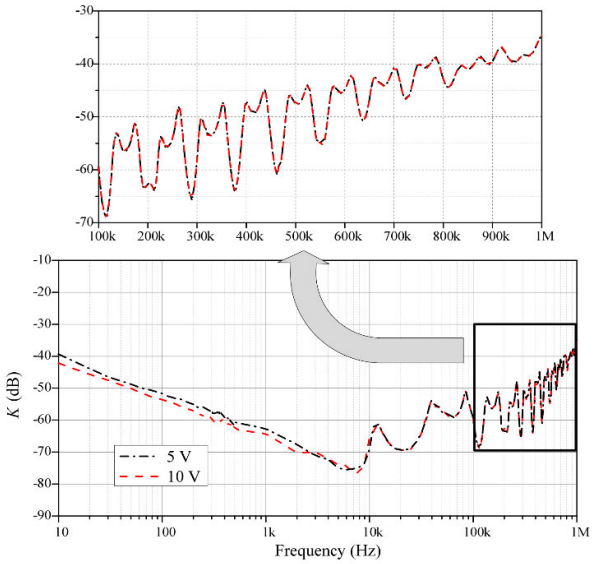


**FIGURE 14. Comparison of FRA curves for two different input voltage values [52].**

Considering the advantages and disadvantages of the mentioned methods, SFRA method is usually used to analyze the transformer frequency response.

### C. SELECTION OF THE APPROPRIATE VOLTAGE AMPLITUDE FOR THE SFRA TEST

As mentioned earlier, in the SFRA analysis, a sinusoidal signal with a low amplitude, from low frequencies to high frequencies, is applied as a reference signal to the transformer. This section discusses why a sinusoidal signal with a low amplitude and close to zero is applied to the transformer. FIGURE 14 shows the frequency response curve of the transformer for the EEOC configuration and two different input amplitudes (5 and 10 volts). As can be seen, the frequency responses differ only until the first anti-resonance frequency (less than 10 kHz) is reached. After that point, the responses match each other. Before the first anti-resonance frequency, there is only an inductive effect with resistance (no capacitive effect is seen). Since the applied voltages are much lower than the nominal voltage of the transformer, the core losses can be ignored, and the equivalent circuit considered as inductance. According to the magnetization curve of the core and the magnetic permeability coefficient shown in FIGURE 15, the operating point G is for applying 5 volts and operating point J is for applying 10 volts. There is a significant difference in magnetic permeability coefficient values between these two points. In fact, there is a direct correlation between the input voltage amplitude and the permeability of the transformer core. Therefore, with a slight change in the input voltage amplitude from 5 to 10 volts and while the transformer is healthy, the inductance experiences significant changes.

This change in inductance leads to a change in the frequency response of a healthy transformer, and it is wrongly assumed that a fault has occurred inside the transformer, while the transformer is healthy. However, if the input voltage amplitude is close to zero, inductance changes can be ignored for small changes in the input amplitude. It is worth noting

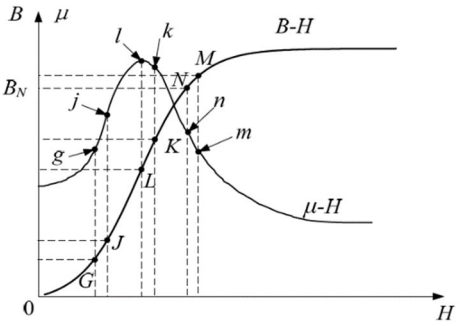


**FIGURE 15.** Iron core's magnetization curve with its magnetic permeability coefficient [52].

that from the first anti-resonance frequency onwards, this problem will not exist for a change in the input voltage amplitude [52].

In relation to the low voltage amplitude applied for the SFRA test, it should also be noted that if the voltage amplitude is too low, the response may be affected by ambient noise and impair performance [51]. Fortunately, the analyzer can solve this problem by increasing the number of measurements (repetitions) and eliminating the noise.

### D. TRANSFORMER FRA IN THE HEALTHY STATE

The FRA method relies on comparing the frequency response of a transformer in both healthy and faulty states. Therefore, it's crucial to have the precise frequency response of the healthy transformer, which is called fingerprint of the available transformer.

Because without access to the fingerprint of the transformer, it is almost impossible to detect the fault type, severity and the location. There are three different approaches to achieve the frequency response of a healthy transformer, which are discussed as follows [53].

1) Time-based approach: This approach is the most accurate and reliable method to obtain the frequency response of a healthy transformer (fingerprint). In this case, the fingerprint is obtained from the previous FRA test data, when it is ensured that the transformer is free of any defects and faults (e.g., right after the installation of the transformer). Since this information is usually rarely available, two other methods are used.
2) Construction-based approach: Due to the symmetrical property that exists in the construction of some three-phase transformers, the result of performing the FRA test on other phases of the transformer can be used as a fingerprint. It should be noted that this similarity is not enough for evaluation in transformers with zigzag coupled windings.
3) Type-based approach: If the fingerprint of the transformer is not available through the above two methods, it is possible to use the FRA test results of similar transformers in terms of design and construction that were produced in the same factory. Due to the existence of tolerance in manufacturing, various statistical evaluation methods are provided, with the help of which, the effect of the design and construction process is separated from the effect of defects and failures.

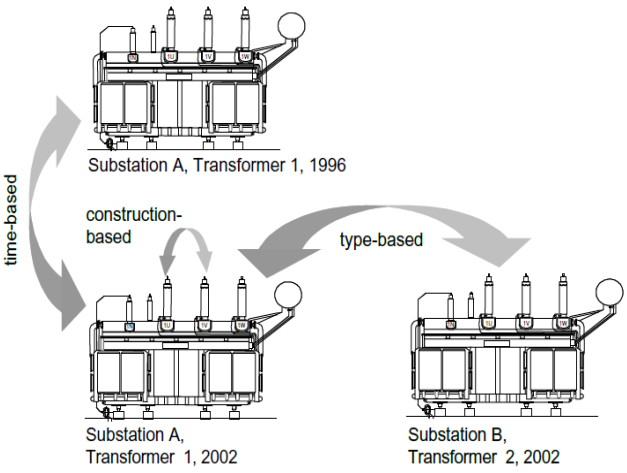


**FIGURE 16.** Different methods for measuring the frequency response of the healthy transformer [53].

These three methods are summarized in the FIGURE 16.

### E. FAULT SEVERITY DETECTION IN CASE OF LACK OF ACCESS TO THE FINGERPRINT

The FRA test involves comparing the frequency response of a transformer in two states: healthy and faulty, for a specific configuration. In some cases, the frequency response of a healthy transformer is not available. In this situation, some methods have been presented in the references to identify the fault without using the frequency response of the healthy transformer and comparing it with the frequency response of the defective transformer.

For instance, reference [54] proposes a method is proposed in which the frequency response of the transformer is compared in a faulty state for different configurations (standard configurations, i.e. EE, EESC, CIW and IIW) with each other, the severity of the mechanical fault can be detected. This reference uses two indicators, including CC and Euclidean distance (ED) to evaluate and compare the frequency response of the defective transformer for two configurations EEOC and EESC and for axial displacements (AD) and radial deformations (RD) faults. In this regard, this result has been obtained that with the increase in the fault severity, the values of the mentioned indicators change monotonically. Hence, the fault severity can be identified with this method. Also, by comparing the frequency response of the transformer for CIW and IIW configurations, a similar result has been obtained.

## IV. INVESTIGATION AND INTERPRETATION OF FREQUENCY RESPONSE

Various factors can lead to faults and changes in the transformer frequency response, including: inter-turn short-circuit fault, DSV fault, AD fault, RD fault, bushing fault, etc. This section will first discuss various methods of analyzing FRA

results, followed by an introduction on the methods that come along with FRA method and cover its weaknesses. Subsequently, it will examine the effect of several important factors on the transformer frequency response, including the type of winding, the important issue of selecting the frequency range for FRA and its sub-ranges as well as the effect of different faults on equivalent circuit parameters. It is also shown that different faults will mainly affect which of the identified sub-ranges of frequency. Finally, the online FRA method is discussed and a comparison with the offline method is presented as well.

### A. DIFFERENT METHODS OF INTERPRETING FRA RESULTS

The comparison of the frequency response of the transformer in both healthy and defective states and its interpretation can be done by an expert through visual inspection. Reference [55] the frequency response of a transformer for open circuit and short circuit faults is examined to develop a guideline approach. The reference discusses the interpretation and analysis of frequency response based on human experience, which may not always be accurate, as operators may not have the necessary skills to evaluate the results in some cases. To address this, researchers have developed methods to remove the human interface, which is going to be discussed in the following subsections.

Each of the following FRA interpretation methods has advantages and disadvantages. One of the drawbacks of FRA analysis as a fault detection tool is that there is no specific procedure and standard for analyzing and interpreting the measurements. Reference [56] compares and states the advantages and disadvantages of some of the methods mentioned below.

#### 1) MODEL-BASED FRA

Reference [57] deals with identifying the fault location based on the synthesis of a lumped-parameter ladder network. For this purpose, the impedance of the excitation point is measured by performing the FRA test for the healthy transformer and based on it, a lumped-parameter ladder network is synthesized using an iterative algorithm, which in this case is called a ''reference circuit''. After a fault occurs, a new circuit is synthesized again, and by comparing its elements with the elements of the reference circuit, the fault location and severity is determined. The results indicate the high accuracy of this method in fault detection. In [41], by extracting the transformer model in both healthy and fault states, the location of various faults such as disc deformation, winding short circuit, aging of insulation, etc. has been well identified. In [26], based on an iterative algorithm, it deals with the synthesis of the transformer ladder model based on the measured excitation point impedance, before and after the fault occurs. Then, based on changing the parameters of the ladder model, the fault type, severity, and location have been identified. The good performance of the mentioned method in fault detection has also been confirmed in [57]. In [39], using the low and medium frequency models of the transformer, the fault involving the magnetic core and its severity have been correctly identified. In [58], based on the improved lumped circuit (ILC) model, the changes in energy transfer and distribution in the elements of the mentioned model for inter-turn fault and its effect on the frequency response of the transformer have been investigated. Short circuit resistance plays a key role in changing the frequency response when a short circuit occurs between the turns of the coil. Because it causes a change in the path of energy transfer between adjacent turns, which increases the resonance frequencies. On the other hand, due to the increase in losses in the transformer winding, it leads to a change in the frequency response amplitude at resonance frequencies. The results show that by reducing the short circuit resistance between the winding turns, the frequency response amplitude at the resonance frequencies experiences a U-shaped trend and also, the resonance frequencies increase. Reference [59] examines the frequency responses of the windings of a single phase transformer with a large voltage ratio. It also approximates the first anti-resonance frequency of the FRA diagrams of the low voltage (LV) and high voltage (HV) windings and highlights the relationships between FRA properties and the electrical components in the equivalent circuit network. The derived results present an intuitive quantitative relationship between the values of the electrical winding components and the corresponding FRA characteristics.

**TABLE 2. Transformer model parameters and its associated mechanical faults [21].**

| Parameter | TYPE OF FAULT |
|---|---|
| Self / Mutual Inductance | Winding / Core deformation, shorted turns and disk space variation |
| Shunt Capacitance | Disk space variation, winding buckling and loss of clamping pressure |
| Series Capacitance | Insulation degradation and disk movement |
| Resistance | Shorted turns |

TABLE 2 illustrates the relationship between the parameters of the electrical model of the transformer and the mechanical faults [21]. In other words, based on this table, it is shown that each of the mechanical faults of the transformer leads to the change of which of the parameters of the model.

#### 2) FRA BASED ON STATISTICAL INDICATORS

In order to remove the operator from the process of analyzing the results of FRA, it is possible to compare the frequency responses in two healthy and defective states using statistical indicators. In this section, by introducing different statistical indicators, it is tried to interpret the results of FRA and make a comparison between these indicators. Various indicators can be used for this purpose, which are presented in TABLE 3 [60].

In connection with the discussion of indicators, their sensitivity, monotonicity and linearity are crucial for the changes in fault severity. Because it is only in this way that it is

**TABLE 3. Different statistical indicators to analyze FRA results [60].**

| Indicators | Descriptions |
|---|---|
| average | $\bar{x} = \frac{\sum x_i}{N}$ |
| quartiles | $x_1, x_1, \ldots, x_N$ are the values sorted from the lowest to the highest. Now Quartile 0 will be the smallest value which satisfies Alldata ≥ QUARTILE0. To obtain Quartile$_z$ ($z$ = 1, 2, 3, 4), if $(z/4)(N+1)$ is integer, the first quartile is $x_{(z/4)(N+1)}$, else Quartile$_z$ is equal to $x_{\text{integer}((z/4)(N+1))} + x_{\text{integer}((z/4)(N+1))+1} \times \text{decimal}((z/4)(N+1))$ |
| median | $M = L + (((N/2) - cf)/f) \times h$ |
| harmonic mean (HAR) | $\frac{1}{\text{HAR}} = \frac{1}{N}\sum_{i=1}^{N}\left(\frac{1}{x_i}\right)$ |
| range | $\text{Range} = \max(x_i) - \min(x_i)$ |
| average deviation (AVEDEV) | $\text{AVEDEV} = \frac{\sum \lvert x_i - \bar{x} \rvert}{N}$ |
| variance | $\sigma^2 = \frac{\sum (x_i - \bar{x})^2}{N}$ |
| standard error of mean (SEM) | $\sigma_{\bar{x}} = \frac{\sigma}{\sqrt{N}}$ |
| relation dispersion (RD) | $\text{RD} = 100 \times (\sigma/\bar{x})$ |
| standard deviation (SD) | $\text{SD} = \sqrt{\frac{1}{N-1}\sum_{i=1}^{N}(x_i - \bar{x})^2}$ |
| skewness (SKEW) | $\text{SKEW} = (3(\bar{x} - \text{AVEDEV}))/\sigma$ |
| kurtosis (KURT) | $\text{KURT} = \left\{\frac{N(N+1)}{(N-1)(N-2)(N-3)}\sum\left(\frac{x_i - \bar{x}}{\text{SD}}\right)^4\right\} - \frac{3(N-1)^2}{(N-2)(N-3)}$ |
| covariance (COVAR) | $\text{COVAR}(x, y) = \frac{1}{N}\sum_{i=1}^{N}(x_i - \bar{x})(y_i - \bar{y})$ |
| correlation coefficient (CC) | $\text{CC}(x, y) = \frac{\sum_{i=1}^{N}(x_i - \bar{x})(y_i - \bar{y})}{\sqrt{\sum_{i=1}^{N}(x_i - \bar{x})^2 \sum_{i=1}^{N}(y_i - \bar{y})^2}}$ |
| absolute sum of logarithmic error (ASLE) | $\text{ASLE} = \frac{\sum_{i=1}^{N} \lvert 20\log_{10}\lvert x_i \rvert - 20\log_{10}\lvert y_i \rvert \rvert}{N}$ |
| absolute average difference (DABS) | $\text{DABS} = \frac{\sum_{i=1}^{N}\lvert x_i - y_i \rvert}{N}$ |
| min–max (MM) ratio | $\text{MM} = \frac{\sum_{i=1}^{N}\min(x_i, y_i)}{\sum_{i=1}^{N}\max(x_i, y_i)}$ |

'$N$' represents the overall size of the data set
'$x_i$' and '$y_i$' represents the overall of all variables present in the data set
'$\bar{x}$' and '$\bar{y}$' are the mean values of observations
'$L$' is lower limit of median class
'$cf$' shows cumulative frequency of class prior to median class
'$f$' is the frequency of median class and '$h$' shows class size

possible to identify the fault type, severity and location based on the indicator value.

Reference [60] introduces and examines statistical indicators and, statistical tests are applied to FRA records in normal and faulty conditions in order to interpret the results of applying SC fault for different severities. Examination and comparison of statistical indicators and statistical tests are divided into two subsections. Once, the statistical indicators and statistical tests are applied for the whole frequency range and in the second case, the whole frequency range is divided into four decade frequency bands and statistical indicators and statistical tests are calculated in these four bands. This action leads to increasing the sensitivity of the indicators and of course, improving their performance in fault detection. Because different faults do not necessarily affect the whole frequency range and only affect certain intervals of it. The results indicate that DABS, which is introduced in TABLE 3, F-test and T-test indicators, which are detailed introduced in [60], are more sensitive in detecting transformer winding faults, among which F-test, due to its greater sensitivity, can well reflect the difference between two healthy and faulty states. In [61], the inter-turn fault and the interpretation of FRA have been investigated based on two indicators, CC and spectrum deviation (SD).

In this case, similar to reference [60], the entire frequency range in the FRA test is divided into four decade frequency bands and the mentioned indicators are calculated in each of these four bands. The following outcomes have been obtained:

- The lowest amount of correlation corresponds to the lowest frequency band. Because for the inter-turn fault, the frequency response changes in this band are more.
- Reliability and sensitivity of SD indicator in detecting inter-turn fault is more than CC indicator. Because with the increase in the severity of the mentioned fault, the shape of the frequency response is almost constant, but the resonance frequencies are moved to higher frequencies, which is mentioned in the reference [60] about the weakness of the CC indicator in such a case.

Reference [62] tries to find the best indicator in terms of sensitivity, capability and reliability by examining different indicators. For this purpose, CC, ASLE, DABS and MM indicators are first introduced to interpret FRA. In this case, the entire frequency range of the FRA test is divided into three-decade bands and the values of these indicators are calculated in each of these frequency bands. The results show that ASLE and MM indicators are more confident and reliable in order to identify faults and make decisions, compared

to CC and DABS. The weakness of the CC indicator has also been confirmed in [60] and [61]. Reference [13] also compares the three indicators, namely CC, SD and ASLE, for detecting minor AD and RD faults. The study demonstrates that the SD and ASLE indicators outperform the other in identifying these faults. Moreover, the effectiveness of the SD indicator is further confirmed by the findings of [60]. Reference [63] also introduces weight functions $F_a$ and $F_f$ as follows:

$$F_a = \sum_j \frac{a_{2j}}{a_{1j}} \times w_{aj} \tag{5}$$

$$F_f = \sum_j \frac{f_{2j}}{f_{1j}} \times w_{fj} \tag{6}$$

In the above equations, $a_{1j}$ and $a_{2j}$, are the transformer frequency response amplitude, before and after the displacement of the $j$th resonance frequency, respectively. The values of $f_{1j}$ and $f_{2j}$ are the $j$th resonance frequency before and after displacement due to AD fault in the transformer, respectively. Furthermore, $w_{aj}$ and $w_{fj}$ are the weighted coefficients of the $j$th resonance frequency for amplitude and frequency, respectively. These two indicators are used to interpret the FRA test and the results show that this approach, independent of the defined transfer function, is a reliable method to evaluate the FRA test. In [64], different indicators of sum squared error (SSE), sum squared ratio error (SSRE), sum squared max-min ratio error (SSMMRE), CC and ASLE are compared for different faults that the results indicate high accuracy of the ASLE indicator. The high capability of the ASLE indicator in fault detection is also confirmed in [13] and [62]. Similarly, in [65], it is concluded that CC and MM indicators are not sensitive to the variation between normal and short circuit conditions, and conversely, ASLE, MSE and SD indicators are sensitive and show a trend due to fault. The reference [66] by introducing the R-square technique, which is based on two indicators, sum of squares of the regression (SSR) and total sum of squares (SST), shows that this methodology performs better in comparison with cross correlation coefficient (CCF) for vertical displacement problems of deviations.

Reference [67] examines and compares CC, MSE, ASLE, MABS, MM and SD indicators for inter-turn fault and radial displacement. Again, in order to increase the sensitivity, the entire frequency range is divided into three-decade bands. The results show that:

- For the inter-turn fault, all indicators in the first band and all indicators except MM in the second band had an acceptable performance.
- For the radial displacement fault, all indicators except MM have a positive performance to identify the fault in all frequency bands. Also, the values of the indicators in the second band have more deviations compared to the first and third bands.

In reference [68], the objective is to identify the location and extent of the RD fault. The study reveals that when a fault occurs, the direction of the shift of the frequency response amplitude at resonance frequencies can be used as an indicator to identify the fault location. Consequently, the RD fault location can be determined using this method. The authors of the reference propose the use of the index of frequency deviation (IFD) and the index of magnitude deviation (IMD), to assess and identify the fault severity. But since these indices are not always proportional to the degree of deformation, SD index, as its proper performance has been confirmed in [13], [61], and [67], has been used to determine the fault severity.

Reference [69] compares the reliability and sensitivity of several indicators, including standardized difference area (SDA), correlation factor ($\rho$), indices of frequency and amplitude deviation (IFD and IAD), weight functions ($W_a$, $W_f$), SD, weighted normalized difference (WND), and stochastic spectrum deviation ($\sigma$), in identifying the fault type, severity and location for disc-space variation (DSV), AD and RD mechanical faults. In order to increase the sensitivity of the mentioned indicators, the entire frequency range has been divided into three bands and the following results have been obtained:

- The SDA indicator shows an irregular behavior in relation to the fault type, severity and location, and therefore, it is not suitable for the interpretation of FRA.
- The correlation factor indicator also has less reliability than other indicators to identify the fault level, which has been confirmed in [60], [61], and [62].
- $W_a$ and $W_f$ indicators are able to identify the fault location and severity. The high capability of these two indicators is also confirmed by [63].

Reference [70] deals with determining the location of the inter-turn fault by using the absolute sum of logarithmic error (ASLE) indicator. The study considers two transfer functions, namely transfer voltage and input impedance, to perform the FRA test. The results show that when the fault location changes from the inner layers to the outer layers of the coil, the values of the ASLE indicator changes in the form of a symmetrical pattern (for the input impedance transfer function) or in the form of a decreasing trend (for the voltage transfer function). Therefore, the mentioned indicator can identify the fault location very well, as mentioned in the references [13] and [62] about the reliability and appropriate sensitivity of this indicator to identify the fault.

In previous references, in order to increase the sensitivity of statistical indicators, the entire frequency range of the FRA test is divided into smaller bands and the presented indicators are calculated in each of these bands. Reference [71] seeks to identify specific frequency bands in which the frequency response changes are proportional to the fault severity. In other words, suppose $TF_{base}$ is the transformer frequency response in a healthy state and $TF_i$ is the frequency response of the faulty transformer. In this case, the difference between these two frequency responses is equal to [71]:

$$\Delta TF_i = TF_{base} - TF_i \tag{7}$$

This reference intends to find bands of the frequency spectrum of the FRA test in which $\Delta TF_i$ can be written in the form of a monotonic function relative to the fault severity. Such frequency ranges are called diagnostic bands. Therefore, it is recommended to interpret and analyze the frequency response in these bands.

Until now, various numerical indices have been employed for interpreting FRA. Although these indicators are straightforward and their implementation is easily possible, they have two drawbacks. First, researchers have not provided explanations about the origin of these indices. Secondly, most of these indicators do not show regular and linear behaviors [72]. Reference [72] uses a probabilistic reasoning to extract the ED indicator, which can identify the fault type and severity.

First, a comparison is made between the ED indicator and other indicators such as correlation coefficient, weight functions, etc., and the results show that the ED indicator is more linear than other indices in detecting the severity of AD and RD faults.

Also, in order to detect the fault type, first the entire frequency range is divided into several frequency bands and the ED indicator is calculated in each of these frequency bands, which is called regional Euclidean distance (RED). The ratio of maximum ED to minimum ED, which is called MMR, can act as a discriminator between AD and RD faults.

The aforementioned indicators were only applied to the frequency response amplitude. References [8] and [73] show that the use of frequency response phase data in the calculation of indices improves their performance in fault detection. For this purpose, the CC and ED indicators were applied to the real and imaginary parts of the frequency response and the results show that this action has led to an increase in the sensitivity of these indicators. Also, by introducing the complex distance (CD) indicator, these references show that this indicator has more sensitivity than other indicators. In fact, the CD indicator calculates the complex distance between samples of two frequency responses by simultaneously using data related to the amplitude and phase of the frequency response, while the ED indicator only calculates the Euclidean distance between the amplitude samples of two frequency responses. It is worth mentioning that the sensitivity of the CD indicator is even higher than the sensitivity of the ED-real part and ED-imaginary part indicators, as shown in FIGURE 17. Finally, reference [8] shows that the CD indicator performs better than the ED indicator in terms of uncertainty.

Reference [74] further explores and compares different indicators and configurations of the FRA test, especially from their influence of uncertainties point of view. In this reference, the indicators of standard deviation (SD), integral of absolute difference (IA), absolute sum of logarithmic error (ASLE), root mean square error (RMSE), standard deviation ($\sigma_e$), stochastic spectrum deviation ($\sigma$), SSE, SSRE, and SSMMRE are taken into account.

The results show that the end-to-end configuration with SSE and $\sigma_e$ indicators are less subject to uncertainties.

In [75] and [76], statistical indicator-based boundary conditions for various operational states of transformers, i.e. normal, suspicious, and critical, are explored using a pattern recognition-based method, named bolstered error estimation, and the level of confidence in decisions made are also estimated. The aim of [77] is to try to collect all the indicators in a single context, compare and classify them based on their characteristics and introduce more appropriate indicators as standard indicators. This reference also defines some criteria for a suitable index such as monotony, linearity, sensitivity, dependence on data points and index ratio. In [78], experimental FRA measurements are performed under various faults. It is concluded that some faults, e.g., inter-disk and short circuit, affects the FRA response at medium and high frequency ranges, while some other faults, e.g. axial winding displacement, radial deformation, and winding bushing fault, affects the FRA response at high frequency range. Besides that, the loss of clamping pressure displays an effect across the entire frequency range. The results also indicates that the ASLE, along with other investigated indicators, performs well in detecting small variations. Reference [79] utilizes bootstrap sampling technique to simulate the effect of many experiments and overcome the difficulty of limited available measured data in FRA interpretation and classification, through establishing a large set of statistical indicators-specific decision boundaries.

Reference [80] proposes an innovative fault segmentation and localization technique based on FRA data. This technique is based on regression analysis. The proposed scheme specifies different transformer conditions, such as healthy windings, axial and radial winding deformations, core deformation and electrical faults.

Reference [81] emphasizes the importance of clustering and optimization methods to improve the performance of the current FRA interpretation. In this regard, this reference extracts the necessary features from the measured transfer functions of various healthy and faulty transformers. Then, using the interval maximum to global maximum (IMGM) indicator and employing the $k$-means method, the collected data are sorted into different clusters and the centers of the clusters are determined using the grasshopper optimization algorithm (GOA). At the end, the distance of the new data from the centers of the sorted clusters is determined and the closest cluster to the new data determines the condition of the transformer. Reference [82] deals with sensitivity analysis of amplitude, phase, real and imaginary components of transfer function for different faults. Moreover, the accuracy of different indicators and four different components of transfer function is investigated. The conclusion drawn from the analysis is that in comparison with the amplitude, the phase, imaginary, and real components of transfer function have more sensitivity to the faults, respectively, and

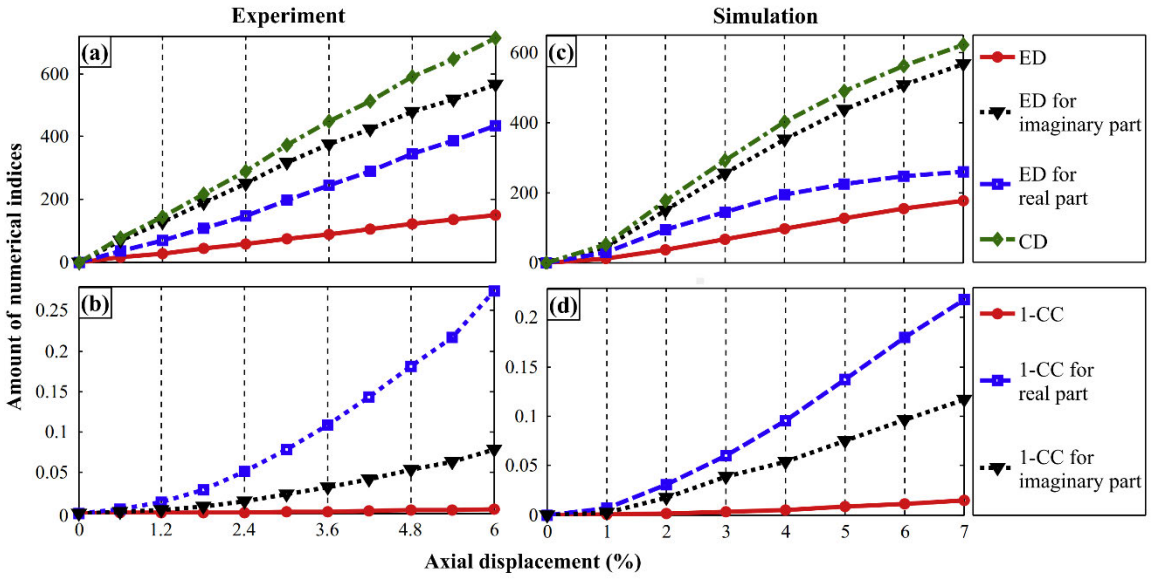


**FIGURE 17.** Comparison of different numerical indicators versus axial displacements for: (a, c) the inductive inter-winding and (b, d) the capacitor inter-winding connections. (a, b) are experimental results whereas (c, d) are simulation results [8].

are more accurate for classification which is confirmed in references [8] and [73].

### 3) FRA BASED ON TRANSFER FUNCTION ESTIMATION

The method of determining the fault type, severity and location by estimating the transfer function is also possible. The estimation-based approach is presented and discussed in this section. In [83], an attempt has been made to determine the location and extent of the RD fault by using the estimation of the transfer function of the transformer. The fault detection process is shown in FIGURE 18. First, using the transformer model, the RD fault is simulated in various locations and for different severities. Then, the transfer function of the transformer is estimated in the form of a rational function in two states, healthy and fault, using the VF method. In this case, the Nyquist diagram can be drawn for the occurrence of faults in various places. Then, based on the shift direction of the Nyquist diagram, a feature is extracted for the occurrence of faults in different places. Based on this feature, the fault location can be identified. After determining the fault location, the fault severity is also calculated based on the sum of absolute displacement of poles (SDP) indicator. This reference states that the SDP indicator has the necessary sensitivity and linearity to identify the fault severity.

In [84], first, the transfer function is estimated in the form of equation (8) for the transformer in two healthy and fault states [84].

$$f_{(s)} = \frac{a_m s^m + \ldots + a_1 s + a_0}{b_n s^n + \ldots + b_1 s + b_0} \tag{8}$$

In this case, by extracting the polynomial coefficients of the numerator and denominator of equation (8), it is possible to calculate the indicator of faulted-intact relation which is shown as equation (9) [84].

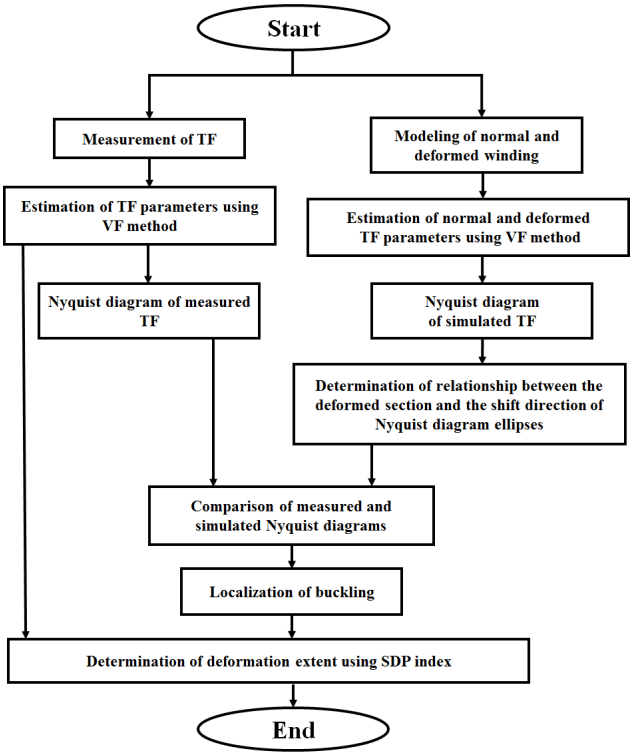


**FIGURE 18.** Algorithm of fault detection mentioned in [83].

$$FI = \left[\frac{\sum_{i=1}^{m} |a_{fi}|}{\sum_{i=1}^{m} |a_{ni}|}\right] \times \left[\frac{\sum_{i=1}^{n} |b_{fi}|}{\sum_{i=1}^{n} |b_{ni}|}\right] \tag{9}$$

In equation (9), $m$ and $n$ are the polynomial degrees of the numerator and denominator of the fraction of the transformation function, respectively.

Also, ($a_{fi}$ and $b_{fi}$) and ($a_{ni}$ and $b_{ni}$) are, respectively, the $i$th polynomial coefficient of the numerator and denominator, mentioned in equation (8), in the faulted condition and the normal condition. In this reference, it has been shown that by using this indicator, the type, severity and location of AD, RD, DSV and SC faults can be detected. On the other hand, by comparing this indicator with the SDP indicator, which is used in [83] to determine the fault severity, it has been concluded that the SDP indicator can hardly identify the fault severity, while the FI index, in addition to estimating the fault severity, has the ability to detect the fault type and location. Reference [85] also calculated the severity of the winding deformation fault by using the estimation of the transfer function and drawing the Nyquist diagram. In this reference, after drawing the Nyquist diagram of the transformer frequency response, in two healthy and defective states, a special feature is extracted from it, based on which the fault severity can be identified. This approach is also confirmed in [84].

The evaluation of this method has also been done on two real transformers and the results show the applicability of this approach for practical use. In [86], with the same approach as those of presented in [85], the location of the inter-disk fault has been detected. The results show that this method has succeeded in identifying the fault location. Reference [27] also deals with the detection of short-circuit fault severity for the transformer inter-turn fault using transfer function estimation. In this reference, the input impedance is well estimated using the VF method. Then, the location of the main pole of the estimated transfer function, which corresponds to the maximum value of the frequency response, has been used as an indicator to identify the fault severity. Reference [87] also uses VF and based on shift of the poles and the zeroes of the frequency response, detects the fault severity in which the principle component analysis (PCA) has been used for this purpose.

#### 4) FRA BASED ON ARTIFICIAL INTELLIGENCE

Artificial intelligence (AI)-based diagnostic methods offer researchers another way to achieve the main purpose of performing FRA. Reference [88] deals with the identification of AD, RD and disc-to-disk short circuit faults. The implementation process is explained as follows. First, the transformer model is extracted considering its specifications and geometric dimensions. Then, the transformer frequency response is obtained in healthy and defected cases. In the next step, based on the frequency response obtained from the previous step, cross-correlation (CC), ED, SSE, and SSRE features are calculated. These features are used for artificial neural network (ANN) training. The results show that this approach has the ability to distinguish the mentioned faults from each other with high accuracy, and also, the fault location and extent are well identified. Block diagram of the mentioned approach is shown in FIGURE 19.

Reference [89] uses a support vector machine (SVM) in order to distinguish AD, RD, DSV and SC faults. In order

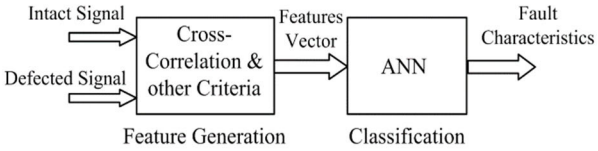


**FIGURE 19.** Block diagram of proposed method in [88].

to improve the classification performance, two different sets of indicators are considered as input to the SVM classifier. In the first set, there are index of frequency ratio (IFR) and index of amplitude ratio (IAR), which are extracted from the frequency response of the transformer in healthy and faulty states. Also, in the second set, there are VF-based indicators which are extracted from the coefficients of the estimated transformation function of the transformer in healthy and faulty states. The results show that the accuracy in the classification of the mentioned faults is higher when the features of the first set are applied as input to the SVM. The study also included a comparison between the SVM classifier and ANN, and the findings demonstrate that SVM provides more precise fault classification for the mentioned faults.

Reference [90] deals with identifying AD, RD, DSV and SC faults. In order to compare the transfer function of the transformer in healthy and faulty conditions, a new method for calculating indicators is proposed, which is called windowed calculated-index (W-index). The basis of this method is that a moving window with a certain length scans the entire frequency range of the FRA test, and the index value (here CC) is calculated in each of these windows. The value of W-index (here W-CC) in each of these windows is used as a feature for fault classification. Therefore, the W-index creates a large number of features per observation. Due to the considerable number of observations and features corresponding to them, the dimensions of the classification problem increase. Using the Linear/Fisher discriminant analysis (LDA/FDA) technique, the dimensions of the problem are reduced and applied to an SVM for classification. The results show that the identification of the fault type, severity and location of occurrence is done with 100% accuracy. Reference [91] also uses fuzzy logic algorithm (FLA) to detect the type of fault and its severity. The results show that this algorithm is able to distinguish different types of faults and their severity from the normal state of the transformer, regardless of the transformer configuration. On the other hand, the low sensitivity of this method to noise makes it a reliable method for this purpose.

Reference [92], considering RD, DSV and SC faults for the transformer winding, uses SVM to identify the fault type and severity. Correlation coefficient, ED, maximum of difference (MAX), integral of absolute difference (IA), SSE, SSRE, SSMMRE and RMSE are applied as input for SVM training, and its parameters are adjusted by PSO algorithm. The obtained results are as follows:

- when the classifier is used as a separator of the mentioned three types of faults, the fault identification accuracy is 96.3%.

- when SVM is used to classify different degrees of DSV fault, its accuracy is 95.24%.
- when SVM is used to discriminate different degrees of RD fault, its accuracy is 70%.

Reference [93] uses machine learning and numerical analysis techniques to train a predictive engine for smart interpretation of FRA data in order to analyze fault severity. The proposed technique, which can be utilized for offline or online application of FRA, is effective for SC inter-turn or inter-disk fault detection and fault severity classification in transformer winding. Reference [94] proposes a two-dimensional Hilbert ID that considers the extraction of a multi-window feature for deep vision fault positioning of the transformer winding. In this regard, sweep frequency response data containing complex fault characteristics are obtained. Also, different intelligent locating methods are compared and the proposed deep vision fault location method is on average 6.51% higher than other methods. In [95], recognized intelligent classifiers, namely probabilistic neural network (PNN), decision tree, SVM, and $k$-nearest neighbors, are utilized to classify transformer faults. Similarly, [96] has utilized SVM, radial basis function (RBF) neural network and statistical $k$-nearest neighbor method for fault classification with different strategies and configurations. Reference [97] divides frequency responses into four frequency ranges based on frequency resonances and anti-resonances, extracts the features of the four frequency ranges by Lin's Concordance Coefficient (LCC) indicator, trains the Multilayer Perceptron (MLP) neural network by the extracted features, and finally, identify and differentiate the types of winding faults.

In reference [98], the machine learning application called generalized regression neural network (GRNN) was used to identify the fault and the results show that the introduced novel index which is called fitting percentage (FP) leads to 100% accuracy of GRNN in RD fault detection. In reference [99], a new methodology based on the combination of SVM and synthetic minority oversampling technique (SMOTE) data preprocessing algorithm is used for fault detection, and the results indicate the high accuracy of this method. Reference [100] also identified the location and severity of the disk space variation (DSV) fault using the self-organizing map (SOM) neural network and shows that this method, like the reference [98], was able to achieve the mentioned goal with a 100% accuracy.

### 5) FRA BASED ON DIGITAL IMAGE PROCESSING

Reference [101] uses the digital image processing (DIP) technique to identify AD and DSV faults using the image of the polar plot of the frequency response of the transformer in two healthy and faulty states. First, pre-processing steps are performed with the aim of adjusting the size and color of the image, as well as image segmentation with the aim of removing unwanted effects including noise. Then, four geometric dimensions features and eleven combined features of invariant moment and texture analysis are extracted from the polar plot image. Then, based on the features extracted from the polar plot image, three indicators city-block distance (CBD), root mean square (RMS) and image Euclidean distance (IED) are calculated. Finally, based on these three indicators, the fault type, severity, and location are identified. The implementation steps of the presented method are shown in FIGURE 20. It is worth noting that the mentioned approach has the ability to identify minor faults, while other common methods have a great weakness in identifying such faults. Reference [102] also used the same approach presented in [101] to detect the severity and location of short circuit faults and the results show that this approach is capable of identifying minor short circuit fault levels. The difference is that instead of AD and DSV faults, reference [102] deals with inter-turns fault.

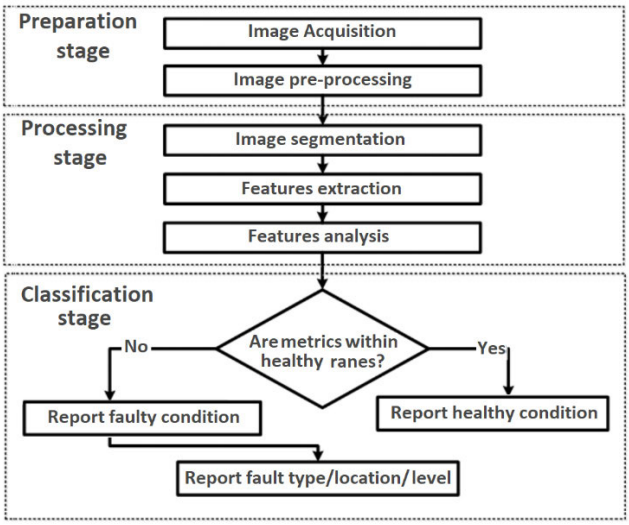


**FIGURE 20.** Flow chart of the presented DIP technique in [101].

By introducing the principles of optical FRA and noise removal and implementing this method, reference [103] takes advantage of its several unique benefits. These benefits include high immunity against electromagnetic interference, direct display of winding deformation, no effect of connected electrical equipment, and high reliability in harsh environments. So, the winding deformation in a power transformer is detected.

### 6) FRA BASED ON DISCRETE WAVELET TRANSFORM

In order to reduce the effect of noise and measurement disturbances, references [6] and [104] present a new approach for fault detection, based on discrete wavelet transform (DWT). The process of this advanced methodology is presented as follows:

- In the first stage, by applying the DWT, the frequency response of the transformer in two healthy and faulty states is decomposed up to seven levels. In this case, seven smoothed versions are extracted.

- Then, starting from the seventh level and reaching the first level, a comparison is made between the smoothed version of present and reference responses. If the difference between the two is greater than a threshold at each level, an abnormal difference is detected, and the corresponding frequency band is stored as an abnormal band. It is worth noting that at lower resolution levels, this frequency band is not scanned again.
- In the next step, the abnormal bands that have been detected at each level are also examined using indicators such as CC and min-max index (MM) to determine whether this abnormality is related to failure or not. This work is done with the aim of increasing the robustness of the presented approach.
- Finally, based on the results of the previous step, the fault type is identified.

The results indicate that this approach is highly reliable in detecting faults, as it effectively removes the effects of noise and disturbances.

### B. FRA SUPPLEMENTARY METHODS

Undoubtedly, no fault diagnosis method for transformers can claim to be perfect and flawless. Every method has its own limitations and weaknesses that can affect its effectiveness in detecting faults accurately. To address these shortcomings, supplementary methods have been proposed and developed over time to improve the accuracy and reliability of transformer fault diagnosis. Some of the main supplementary methods are explained below.

#### 1) IMPEDANCE METHOD

Research shows that the standard FRA assessment cannot always be sufficient to identify faults. Therefore, the reference [32] states that the impedance method (IM), which is based on the low and medium frequency model of the transformer, supports the standard FRA assessment. This reference has investigated the sensitivity of standard FRA and IM for the occurrence of AD and RD mechanical faults. For AD fault, the condition of transformer is reported as normal by EEOC and EESC configurations assessment based on correlation coefficients, while in IM, significant change of leakage inductance and slight change of capacitor between high and low voltages coil indicate the occurrence of fault in transformer. Also, for RD fault, no fault is reported by the assessment of EEOC, EESC, CIW and IIW configurations, while the decrease in the value of earth capacitor in IM indicates the occurrence of RD fault. Finally, it has been concluded that the combination of standard FRA and IM is the best solution for detecting mechanical faults of the transformer winding.

Also in [33], by comparing the changes of the parameters of the transformer ladder model extracted from the FRA standard test and the parameters of the IM model in low and medium frequencies, it has been concluded that, for the AD and RD minor faults, the parameters of the ladder model do not have enough sensitivity to identify mechanical faults. Meanwhile, IM model parameters can be sensitive indicators for this purpose. It seems that using the digital image processing (DIP) method to evaluate and interpret the FRA standard can be a suitable alternative to the two evaluation methods adopted in [32] and [33] for the interpretation of the FRA standard. Because the DIP method is able to identify minor mechanical faults as well [101], [102].

#### 2) CHARACTERISTIC IMPEDANCE

The FRA method is very sensitive to the measuring setup at high frequencies. Also, due to the effectiveness of this method from external factors, reference [105] provides another method to evaluate the condition of the transformer. In this method, considering the transformer winding as a long transmission line, its characteristic impedance ($Z_c$) is obtained as the signature of the transformer. The characteristic impedance of the transformer winding is unique and independent of external factors. Any change in the geometry of the transformer winding due to mechanical faults leads to a change in the $Z_c$ curve at different frequencies. By comparing the $Z_c$ curve of the transformer winding in two healthy and faulty states, it is possible to determine the fault type, severity and location. For this purpose, a sinusoidal signal from low frequencies to high frequencies is applied to the input terminal of the transformer and by measuring the voltage and current in its other terminal, the characteristic impedance is obtained as follows [105]:

$$Z_c = \sqrt{\left| \frac{V_{in}^2(\omega) - V_{out}^2(\omega)}{I_{in}^2(\omega) - I_{out}^2(\omega)} \right|} \tag{10}$$

The wavelet coherence indicator is also used to compare two $Z_c$ curves (before and after the occurrence of the fault). In this reference, two types of faults, AD and RD, are investigated and the results show that the characteristic impedance has a higher sensitivity to the occurrence of small mechanical faults compared to FRA.

#### 3) VIBROACOUSTIC METHOD

In this method, the accelerometer sensor is installed on different parts of the transformer tank and its vibrations are recorded. Reports indicate that, if the shape of the coils does not change while only loosely closed, the FRA method cannot detect the fault; but can be detected by the vibration-based method (VM) [106], [107].

### C. EFFECT OF SEVERAL IMPORTANT FACTORS ON THE TRANSFORMER FREQUENCY RESPONSE

In the following, the effect of some factors such as winding type, transformer structure and some other factors affecting the frequency response are explained.

#### 1) EFFECT OF WINDING TYPE, STRUCTURE AND RESIDUAL FLUX OF TRANSFORMER

In [108], the impact of different winding structures on end-to-end FRA responses has been investigated. In general, the

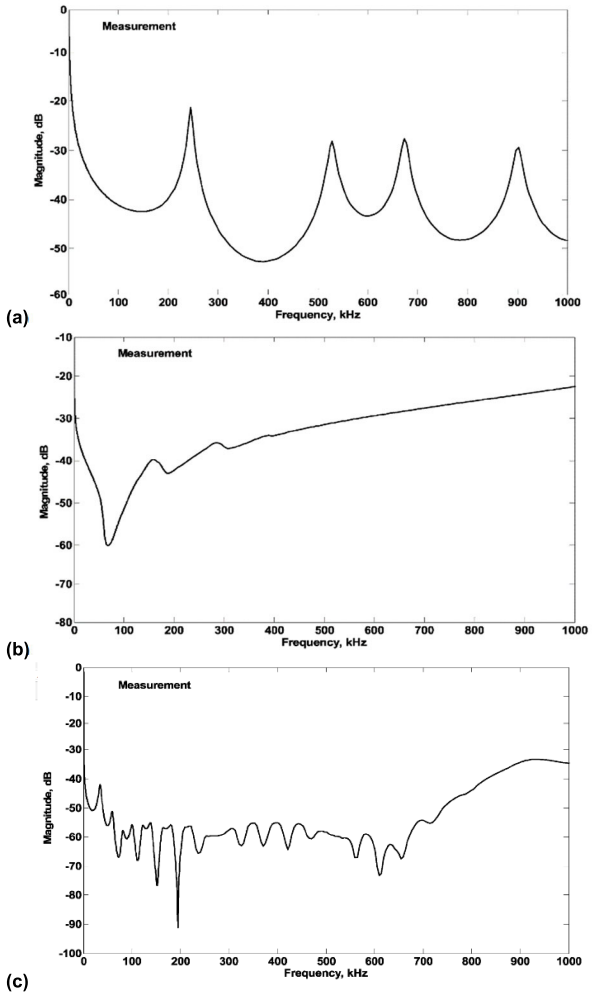


**FIGURE 21.** Frequency response of different windings: (a) Continuous disc winding. (b) Interleaved disc winding. (c) Inter-shielded disc winding [108].

ratio of series capacitance ($C_s$) and shunt capacitance ($C_g$) is very important in determining the FRA response for a specific winding structure because this ratio will determine the shape and position of resonance and anti-resonance frequencies. The results of this research are presented as follows:

- In the frequency response of windings with low $C_s$ value, the stable magnitude trend with a series of well-defined resonances and quasi-resonances is observed. Continuous disc winding is in this category of windings (FIGURE 21-a).
- In the frequency response of windings with high $C_s$ value, the increasing trend of magnitude with little resonances and anti-resonances is seen. Inter-leaved disc-type winding is an example of a winding with high $C_s$ (FIGURE 21-b).
- The frequency response of the inter-shielded disc winding starts with a series of ''U''-shaped resonances and quasi-resonances. Then the response becomes ''camel hump''-shaped with damped resonances and anti-resonances (FIGURE 21-c).

Reference [109] with a more accurate modeling of the transformer winding compared to reference [108] and with a mathematical approach based on the theory of traveling waves, examines the frequency response of two different types of windings, i.e. continuous disc winding and interleaved disc winding, in intermediate frequencies. The results show that at intermediate frequencies, the frequency response of continuous disc winding experiences more oscillations than those of interleaved disc winding. This result is also confirmed in [108]. In addition to the type of transformer phase winding, the interactions between the winding under test and other windings (other windings of the same phase and other phases) in the D-connection state due to magnetic coupling and capacitive effect between them affects the frequency response (resonance and anti-resonance frequencies) [110].

Reference [111] investigates the effect of magnetization condition of the transformer core on FRA measurement. In order to avoid the effects of core magnetization, the FRA test should not be performed immediately after disconnecting the transformer from the power grid. Therefore, the FRA test is recommended to be performed at least 24 hours after the transformer is de-energized. In order to simultaneously remove and measure the residual flux of a three-phase transformer core, reference [112] suggests an improved flux-controlled variable frequency-constant voltage (VFCV) strategy along with the core flux equalization using a low power electronic device.

### 2) EFFECT OF TRANSFORMER TAP CHANGER

Reference [113] investigates the effect of transformer tap changer setting on FRA. The FRA results for open circuit, short circuit and inductive inter-winding configurations clearly show that the tap changer setting influences the frequency response of the transformer in low and medium frequencies. These changes in the frequency response at low frequencies occur due to changes in the inductance of the transformer winding. Therefore, the position of the tap changer should remain constant during the FRA test.

### 3) EFFECT OF TRANSFORMER BUSHING MODELING

In [114], the effect of transformer bushing modeling on its FRA signature has been investigated. In this reference, the transformer bushing is added as a T-model to the transformer ladder model. Considering the bushing model, the resonance frequency of the transformer transfer function at low and medium frequencies do not change. But due to the fact that bushing increases the capacitive components of the transformer, the bushing modeling at high frequencies leads to the change of resonance frequencies and their corresponding amplitudes. Therefore, when modeling the transformer for FRA, the bushing model should also be considered in order to increase the simulation accuracy.

Reference [115] also investigates the effect of bushing fault on FRA signature and in this way determines the minimum failure level that can be revealed visually from FRA response.

It also shows that the impact of the bushing fault appears at high frequencies, which is also confirmed by [114]. In [23], transformer bushing is added as T-model to the transformer hybrid model and by using CC and spectrum deviation ($\sigma$) indices to interpret the results, it is shown that considering the bushing model causes the frequency response to change only at high frequencies. The results of references [114] and [115] also confirm this.

#### 4) EFFECT OF TEMPERATURE AND MOISTURE

References [116] and [117] investigate the effect of temperature and moisture content changes on FRA. Changes in temperature and moisture lead to changes in the transformer frequency response in medium and high frequencies. So that with increasing temperature, resonance frequencies in FRA spectra shift towards lower frequencies and some resonant magnitudes are damped, just like the moisture migration from the paper into the oil insulation when the temperature remained unchanged. Also, with increasing temperature, the increasing trend is evident in the total capacitance variation of transformer windings. In these references, the CC and standard deviation (SD) indicators are used to interpret FRA for changes in temperature and moisture content, and the results show that these indicators do not have sufficient accuracy in interpreting FRA, and therefore they should be modified in some way. Also, in [118] and [119], changes in FRA signature due to temperature changes of transformer conductors and moisture content of its insulation have been investigated. The results show that, regardless of the type of transformer winding, with changes in temperature and moisture, the FRA signature changes have the same pattern. So, with the increase in temperature and moisture, the transformer frequency response shifts in the medium and high frequencies towards the lower frequencies. These results are also confirmed by [116] and [117]. Reference [120] also compares the effect of moisture changes in transformer paper insulation and also winding deformation on the transformer frequency response. Finally, it has been concluded that the effect of moisture migration can be seen in the medium and high frequency bands, but in connection with mechanical defects, this effect can be seen in each or every part of the entire frequency range. A new moisture sensor and measurement method is presented in [121], which is based on the introduction of considering capacitive effects inside the transformer tank and the analysis of its frequency response with the FRA test. The sensor should be immersed in transformer oil, away from high voltage areas. Since the moisture of the oil depends on the temperature, the temperature of the oil must also be measured. Also, reference [122] evaluates the capability and accuracy of its presented method in determining the moisture content of the transformer by obtaining the results of FRA, extracting the required features, using the $k$-means method for placing these features in three clusters (dry, wet, and excessively wet), and optimizing the cost function of the $k$-means method using the PSO algorithm.

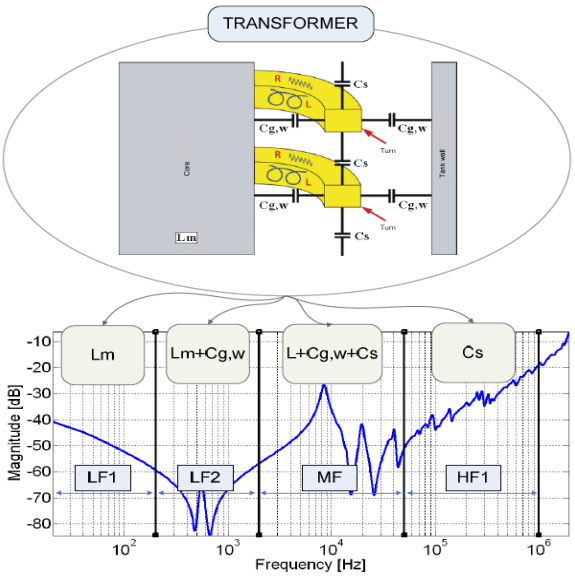


**FIGURE 22.** Frequency range defined by the expert [123].

### D. SELECTION OF THE APPROPRIATE FREQUENCY RANGE FOR THE FRA AND AUTOMATICALLY DETERMINING ITS SUB-RANGES

Although it is generally possible to divide the frequency range into three sub-ranges of low frequency (LF), medium frequency (MF), and high frequency (HF), it is not clear what range of frequencies each of these sub-ranges encompasses. This depends on the structure of the transformer and its configuration, the type of winding and its voltage level, and therefore, a general rule cannot be considered for it [42]. On the other hand, a proper definition of these sub-ranges can improve the capability of the indicators presented earlier. In this section, the following topics are discussed:

- Selection of the appropriate frequency range for FRA testing and the factors affecting the limitation of this range.
- The mentioned frequency spectrum is divided into several different sub-ranges and what frequency range each of these sub-ranges includes.
- Which of these sub-ranges are affected by each of the electrical and mechanical faults and the consequent change in the parameters of the equivalent circuit?

In general, the frequency range can be considered as FIGURE 22 [123]. Based on this figure, the following can be deduced:

1) The LF range itself is divided into two smaller ranges LF1 and LF2. In the LF1 range, only the transformer core magnetic inductance ($L_m$) will have a dominant effect on the frequency response as can be observed from its nearly linear behavior. Since no capacitor is effective in this range, the oscillations in the frequency response occur solely due to interactions mutually with $L_m$ inductance. However, in the LF2 range, due to the interactions between the $L_m$ inductance and the

$C_{g,w}$ parallel capacitors, the combination of these two elements will have a dominant effect in this range.

2) In the MF range, the penetration depth of the magnetic field inside the transformer core is reduced. So, the core behaves like an aerial core with a specific inductance (L). Due to its interactions with series capacitors ($C_s$) and parallel capacitors ($C_{g,w}$) as well as the effect of mutual coupling between the windings ($L_M$) and the capacitor between the high-voltage and low-voltage windings, large fluctuations occur in this range.
3) The HF range is also divided into two smaller ranges, HF1 and HF2. In the HF1 range, series capacitors ($C_s$) will have the predominant effect. In the HF2 range, which is not shown in FIGURE 22 and includes frequencies above 1 MHz, the measurement system also affects the frequency response.

Reference [123] presents an automatic method for determining the mentioned frequency ranges. The principle of this method is based on the resonance frequencies corresponding to passing through the zero phase of the frequency response. In other words, based on the critical points of passing through the zero phase of the frequency response, the proposed method determines the frequency ranges of each sub-range.

Because the number of resonance frequencies and their location change. In this regard, this method can adapt itself to the new conditions and specify frequency ranges. This means that the method is adaptive. FIGURE 23 shows the effect of various electrical and mechanical faults on each of the frequency ranges. The first classification level considers some faults that affect only one frequency range and change the frequency response in that range, denoted by R1, R2, R3, R4, and R5, and corresponding to the LF1, LF2, MF, HF1, and HF2, respectively. The second classification level includes some other faults that affect two adjacent ranges represented by F1, F2, F3, and F4. The third classification level covers general electrical and mechanical faults, denoted by EM and MM, respectively. However, there are some faults affecting all frequency ranges and their interpretation can be based on the behavior of the resonance peak. References [124] and [125] examine the effect of different faults on frequency ranges and present that RD fault affects all frequency ranges, while AD fault affects intermediate and higher frequencies. The effect of SC fault and fault between disks is also evident at low and medium frequencies, respectively. Reference [126] examines the RD fault and models this fault by changing the capacitor between the high voltage and low voltage windings. The results indicate that this type of fault affects the entire frequency range. Actually, the results of [124] and [125] are approved by another method. Reference [127] also obtains a similar result for the RD fault.

Some researchers believe that only the mutual inductance between the high-voltage and low-voltage windings changes when an AD fault occurs. Therefore, they change this parameter in the modeling, so that they can model the AD fault and then, compare the output with the frequency response of the transformer in the healthy state and evaluate different methods to determine its severity.

The authors indicate in [128] that when an AD fault occurs on a high voltage coil, not only the mutual inductance but also the capacitor between the high voltage coil and the transformer body, as well as the capacitor between the high voltage coil and the low voltage coil changes and these changes are evident. Therefore, in AD fault modeling, this point should be considered so that different methods of fault severity detection are evaluated and compared correctly. The authors of references [129], [130], and [131] also believe that the AD fault affects the intermediate frequencies. This type of fault, in addition to changing the inductance matrix of the equivalent circuit, changes the capacitive matrix that changing of these two parameters should be considered to model this type of fault. In [132], it is shown with the same process, for modeling the RD fault correctly, two changes must be considered; changing the values of the equivalent circuit capacitances, and changing the circuit inductance matrix. The effect of this fault is evident in the whole frequency range. In [23], using the hybrid transformer model and optimizing its parameters, the effect of different transformer faults on the frequency response is evaluated and the obtained results indicate that AD and RD faults have their main effect on the medium frequencies (approximately 1 MHz).

### E. ONLINE FRA METHOD

The FRA test requires the transformer to be de-energized and disconnected, and laboratory instrumentation must be used to determine the transfer function. As a result, this may incur high costs and reduce network reliability. This means that this test cannot be carried out repeatedly to implement precautionary actions. It is only performed when the transformer is suspected of being faulty, and corrective actions are taken if necessary. In order to solve this problem, it prompted the researchers to provide methods that detect the internal defects of the transformer without disconnecting it from the power grid and determine the severity of the fault and the location inside the transformer online.

As mentioned earlier, FRA testing (including its online method) can be performed in two ways, SFRA and IFRA. But according to the reports, the online testing has some problems [133], [134]. Some of these difficulties are:

- The moment of applying the FRA signal is very important due to its effect on the obtained frequency response,
- The possibility of interference on network controller signals by reference signal (with frequencies from several Hz to several MHz),
- The possibility of damage to the analyzer device in case of directly connecting it to the transformer,
- The effect of transformer load on online FRA fault detection capability, etc.

Also, several advantages for an online FRA test are worth-mentioning, such as [135]:

- Lower cost of testing,

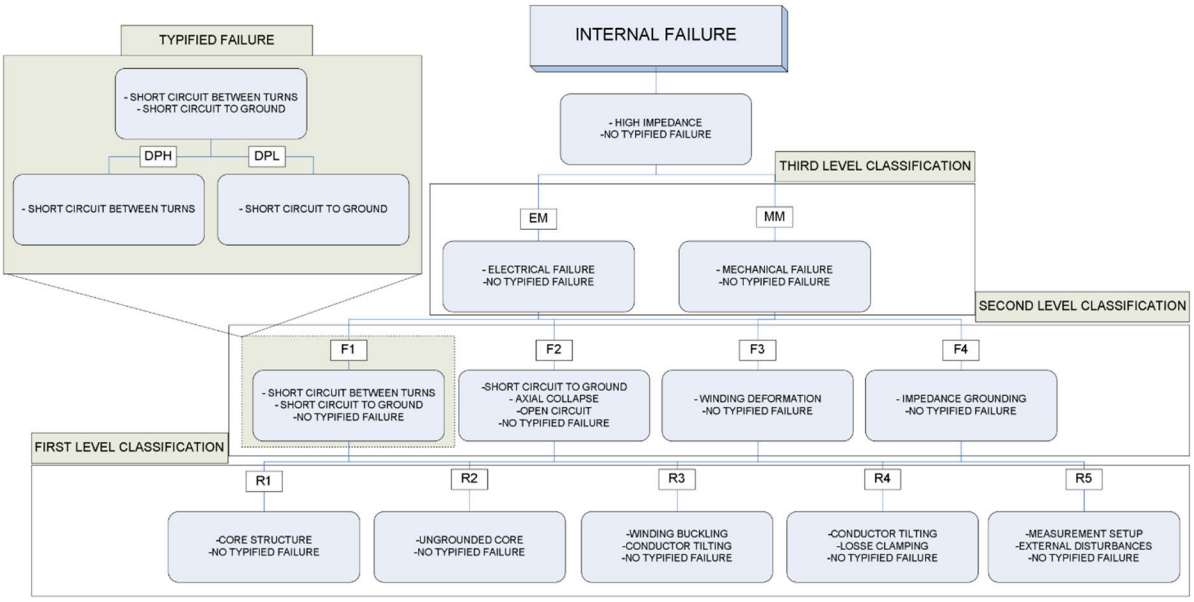


**FIGURE 23.** Classification of fault types inside the transformer [123].

- No requirement for disconnecting the transformer from the grid.

Some researchers have focused on online FRA. For example, references [136] and [137] deal with the effect of transformer load on online FRA fault detection capability. In [138], by utilizing and comparing two methods, IFRA and lightning impulse analysis (LIA), detection of winding deformation and short circuit faults on live transformers is studied. Results show that the diagnosis of transformer windings and detection of incipient faults are possible. Reference [139] explains several online transformer FRA methods, for detecting several faults, specially the inter-turn fault. These methods include (DGA) [140], current harmonic analysis [141], vibration analysis [142], the differential current based on negative sequence and Extended Park Vector [143], [144], $\Delta$V-I locus diagram [145], and flux leakage method [146]. These methods have been usually evaluated qualitatively with a focus on feasibility. In this regard, reference [147] by leveraging both experiment and theoretical analysis, tries to completely evaluate several fundamental aspects of online FRA methods, including sensitivity, repeatability, and anti-interference.

The IFRA method itself can be done in two ways: the controlled and the uncontrolled signal application methods, while the SFRA method is performed only in a controlled manner. In the controlled signal application method, the pulse signal is generated by a pulse wave generator. The advantage of the controlled method is that firstly, the signal application time and secondly, the signal shape and its presence time (which will determine its frequency content) will be controlled and the aforementioned difficulties will be slightly reduced. In the uncontrolled signal application method, lightning or switching signals that occur in the substation are used. The advantage of this method is that there is no need for a pulse signal generator. But the drawback is that firstly these signals are not always available, and one has to wait for a certain moment for one of the two voltage waves to occur and secondly, the shape and duration of presence of such uncontrolled signals are not adjustable.

Reference [148] first deals with the necessary tools to implement the online FRA test and then compares it with the offline one, and shows that in the online FRA due to the presence of noise, the low frequency information of the frequency response cannot be trusted. This makes it challenging to detect the occurrence of faults that affect this frequency range, such as a short-circuit fault.

## V. CONCLUSION AND RECOMMENDATIONS FOR FUTURE IMPROVEMENTS

In this paper, while expressing the need for the importance of transformers in power grids and detecting the occurrence of various faults in it, the frequency behavior of the transformer is explained, and various models are presented to simulate its actual behavior against different frequencies. Moreover, the requirements of FRA for implementation are explained and it is shown that the four configurations named EE, EESC, CIW and IIW together with the transfer voltage, form the best and most sensitive configuration-transfer function pair for FRA. In addition to that, various methods for FRA are examined. After analyzing the FRA results using different methods, complementary FRA methods are introduced and it is shown that three different methods, namely the impedance, the characteristic impedance, and the vibroacoustic methods, can eliminate the weaknesses of the FRA test in order to identify the faults.

The effect of several factors such as winding type, structure, residual flux, temperature and moisture on the frequency

response of the transformer is also investigated and it is shown that some of these factors can significantly change the frequency response. After examining the effect of these factors on the frequency response, it is pointed out that due to the effect of these factors, there is a need for an adaptive and flexible frequency range for FRA. Therefore, using an adaptive method, the frequency range is divided into different sub-ranges in order to increase the sensitivity of statistical indicators to analyze the FRA results. Furthermore, different indicators have been examined from the perspective of sensitivity, capability and reliability. Also, it is shown that each of the electrical and mechanical faults firstly, on which of the specified sub-ranges, have a greater effect, and secondly, each of these faults leads to a change in which of the equivalent circuit elements. Finally, the online FRA method is discussed, and its challenges are mentioned.

The following topics are suggested in order to continue further research in FRA:

- In section IV-A2, it was stated that some indicators do not show a regular and linear behavior with respect to the changes in fault severity, and therefore cannot be useful in determining the fault severity value. Since each fault usually does not affect the entire frequency response range of the transformer and only affects a specific interval of the entire frequency range (which was stated in section IV-D). Therefore, some papers in order to solve this problem recommend the approach of dividing the entire frequency range into several smaller intervals and calculating each of the indicators presented in section IV-A2 in that frequency interval where the specific fault is effective. Because it has been shown that the values of the indicators in the interval of the frequency range where the specific fault is effective, usually show a linear relationship with respect to the changes in the fault severity. The problem that exists is that even with this technique, some indicators still do not experience a linear relationship with the changes in the fault severity. Therefore, to solve this problem, it is suggested to draw the difference function ($\Delta TF_i$) graph presented in equation (7) in that frequency range where the specific fault is effective. Then, in that frequency range, a smaller interval should be found so that the values of $\Delta TF_i$ in that smaller interval have a significant difference with each other, and also the curve-fitting of the $\Delta TF$ diagram according to the severity of different faults, experiences a linear relationship. Such small bands are called diagnostic bands, which was mentioned in section IV-A2. Therefore, the calculation of the indicators in the diagnostic band related to the frequency range where the mentioned fault is effective, can have a significant effect on the linearity and monotonicity of the mentioned indicator.
- In section III-A, it was shown that choosing the appropriate configuration and transfer function to perform the FRA test has a significant effect on increasing the ability to detect faults in this method. Therefore, for a two-winding transformer, many terminal connections were considered and for each terminal connection, different transfer functions were examined. Then, based on the number of natural frequencies appearing in the transfer function, different configuration-transfer function pairs were categorized (TABLE 1). Finally, the configuration-transfer function pair that has the highest natural frequency and, of course, the highest sensitivity for fault detection, was selected for FRA test. Since a large 3-phase transformer as well as multi-winding transformers have more terminals than two-winding transformers, it is possible to define far more terminal connections than a two-winding transformer to perform the FRA test. Therefore, the process mentioned in section III can be implemented in order to find the suitable configuration-transfer function pair to perform the FRA test on this class of transformers.

## REFERENCES


[1] E. Gockenbach and H. Borsi, "Condition monitoring and diagnosis of power transformers," in *Proc. Int. Conf. Condition Monitor. Diagnosis*, 2008, pp. 894–897.

[2] J. N'cho, I. Fofana, Y. Hadjadj, and A. Beroual, "Review of physicochemical-based diagnostic techniques for assessing insulation condition in aged transformers," *Energies*, vol. 9, no. 5, p. 367, May 2016.

[3] M. Badawi, S. A. Ibrahim, D. A. Mansour, A. A. El-Faraskoury, S. A. Ward, K. Mahmoud, M. Lehtonen, and M. M. F. Darwish, "Reliable estimation for health index of transformer oil based on novel combined predictive maintenance techniques," *IEEE Access*, vol. 10, pp. 25954–25972, 2022.

[4] M. M. F. Darwish, M. H. A. Hassan, N. M. K. Abdel-Gawad, and D. A. Mansour, "A new method for estimating transformer health index based on ultraviolet-visible spectroscopy," in *Proc. 23rd Int. Middle East Power Syst. Conf. (MEPCON)*, Dec. 2022, pp. 1–5.

[5] M. M. F. Darwish, M. H. A. Hassan, N. M. K. Abdel-Gawad, and D. A. Mansour, "Application of infrared spectroscopy for discrimination between electrical and thermal faults in transformer oil," in *Proc. 9th Int. Conf. Condition Monitor. Diagnosis (CMD)*, Nov. 2022, pp. 255–258.

[6] J. C. Gonzales Arispe and E. E. Mombello, "Detection of failures within transformers by FRA using multiresolution decomposition," *IEEE Trans. Power Del.*, vol. 29, no. 3, pp. 1127–1137, Jun. 2014.

[7] M. H. Samimi, S. Tenbohlen, A. A. S. Akmal, and H. Mohseni, "Effect of different connection schemes, terminating resistors and measurement impedances on the sensitivity of the FRA method," *IEEE Trans. Power Del.*, vol. 32, no. 4, pp. 1713–1720, Aug. 2017.

[8] M. H. Samimi, S. Tenbohlen, A. A. Shayegani Akmal, and H. Mohseni, "Improving the numerical indices proposed for the FRA interpretation by including the phase response," *Int. J. Electr. Power Energy Syst.*, vol. 83, pp. 585–593, Dec. 2016.

[9] S. D. Mitchell and J. S. Welsh, "The influence of complex permeability on the broadband frequency response of a power transformer," *IEEE Trans. Power Del.*, vol. 25, no. 2, pp. 803–813, Apr. 2010.

[10] K. G. N. B. Abeywickrama, Y. V. Serdyuk, and S. M. Gubanski, "Exploring possibilities for characterization of power transformer insulation by frequency response analysis (FRA)," *IEEE Trans. Power Del.*, vol. 21, no. 3, pp. 1375–1382, Jul. 2006.

[11] A. Shintemirov, W. H. Tang, and Q. H. Wu, "A hybrid winding model of disc-type power transformers for frequency response analysis," *IEEE Trans. Power Del.*, vol. 24, no. 2, pp. 730–739, Apr. 2009.

[12] S. Almas, T. Wenhu, and Q. H. Wu, "Modeling of a power transformer winding for deformation detection based on frequency response analysis," in *Proc. Chin. Control Conf.*, Jul. 2006, pp. 506–510.

[13] W. H. Tang, A. Shintemirov, and Q. H. Wu, "Detection of minor winding deformation fault in high frequency range for power transformer," in *Proc. IEEE PES Gen. Meeting*, Jul. 2010, pp. 1–6.

[14] A. Shintemirov and Q. H. Wu, "Transfer function of transformer winding for frequency response analysis based on traveling wave theory," in *Proc. Int. Control Conf. (ICC)*, 2006, p. 6.
[15] S. D. Mitchell and J. S. Welsh, "Modeling power transformers to support the interpretation of frequency-response analysis," *IEEE Trans. Power Del.*, vol. 26, no. 4, pp. 2705–2717, Oct. 2011.
[16] E. Rahimpour, J. Christian, K. Feser, and H. Mohseni, "Transfer function method to diagnose axial displacement and radial deformation of transformer windings," *IEEE Trans. Power Del.*, vol. 18, no. 2, pp. 493–505, Apr. 2003.
[17] A. Shintemirov, W. J. Tang, W. H. Tang, and Q. H. Wu, "Improved modelling of power transformer winding using bacterial swarming algorithm and frequency response analysis," *Electric Power Syst. Res.*, vol. 80, no. 9, pp. 1111–1120, Sep. 2010.
[18] V. Rashtchi, E. Rahimpour, and E. M. Rezapour, "Using a genetic algorithm for parameter identification of transformer R-L-C-M model," *Electr. Eng.*, vol. 88, no. 5, pp. 417–422, Jun. 2006.
[19] P. Mukherjee and L. Satish, "Construction of equivalent circuit of a single and isolated transformer winding from FRA data using the ABC algorithm," *IEEE Trans. Power Del.*, vol. 27, no. 2, pp. 963–970, Apr. 2012.
[20] V. Rashtchi, H. Shayeghi, M. Mahdavi, A. Kimiyaghalam, and E. Rahimpour, "Using an improved PSO algorithm for parameter identification of transformer detailed model," *Int. J. Electr. Power Energy Syst.*, vol. 1, no. 3, pp. 138–144, 2008.
[21] A. Abu-Siada, M. I. Mosaad, D. Kim, and M. F. El-Naggar, "Estimating power transformer high frequency model parameters using frequency response analysis," *IEEE Trans. Power Del.*, vol. 35, no. 3, pp. 1267–1277, Jun. 2020, doi: 10.1109/TPWRD.2019.2938020.
[22] M. M. Shabestary, A. J. Ghanizadeh, G. B. Gharehpetian, and M. Agha-Mirsalim, "Ladder network parameters determination considering nondominant resonances of the transformer winding," *IEEE Trans. Power Del.*, vol. 29, no. 1, pp. 108–117, Feb. 2014.
[23] T. Y. Ji, W. H. Tang, and Q. H. Wu, "Detection of power transformer winding deformation and variation of measurement connections using a hybrid winding model," *Electric Power Syst. Res.*, vol. 87, pp. 39–46, Jun. 2012.
[24] S. Pramanik and L. Satish, "Estimation of series capacitance of a transformer winding based on frequency-response data: An indirect measurement approach," *IEEE Trans. Power Del.*, vol. 26, no. 4, pp. 2870–2878, Oct. 2011.
[25] K. Ragavan and L. Satish, "Construction of physically realizable driving-point function from measured frequency response data on a model winding," *IEEE Trans. Power Del.*, vol. 23, no. 2, pp. 760–767, Apr. 2008.
[26] K. Ragavan and L. Satish, "Localization of changes in a model winding based on terminal measurements: Experimental study," *IEEE Trans. Power Del.*, vol. 22, no. 3, pp. 1557–1565, Jul. 2007.
[27] R. M. Youssouf, F. Meghnefi, and I. Fofana, "Frequency response analyses via rational function fitting," in *Proc. Annu. Rep. Conf. Electr. Insul. Dielectric Phenomena*, Oct. 2012, pp. 230–233.
[28] M. Heindl, S. Tenbohlen, A. Kraetge, M. Krüger, and J. Velásquez, "Algorithmic determination of pole-zero representations of power transformers' transfer functions for interpretation of FRA data," in *Proc. 16th Int. Symp. High Voltage Eng.*, Johannesburg, South Africa, 2009, P. D-26.
[29] D. A. K. Pham, T. M. T. Pham, V. N. C. Ho, H. Borsi, and E. Gockenbach, "Duality-based lumped transformer equivalent circuit at low frequencies under single-phase excitation," in *Proc. Int. Conf. High Voltage Eng. Appl.*, Sep. 2012, pp. 600–603.
[30] D. A. K. Pham, T. M. T. Pham, H. Borsi, and E. Gockenbach, "A new method for purposes of failure diagnostics and FRA interpretation applicable to power transformers," *IEEE Trans. Dielectr. Electr. Insul.*, vol. 20, no. 6, pp. 2026–2034, Dec. 2013.
[31] D. A. K. Pham, T. M. T. Pham, M. H. Safari, V. N. C. Ho, H. Borsi, and E. Gockenbach, "FRA-based transformer parameters at low frequencies," in *Proc. Int. Conf. High Voltage Eng. Appl.*, Sep. 2012, pp. 476–479.
[32] D. A. K. Pham, T. M. T. Pham, H. Borsi, and E. Gockenbach, "A new diagnostic method to support standard frequency response analysis assessments for diagnostics of transformer winding mechanical failures," *IEEE Elect. Insul. Mag.*, vol. 30, no. 2, pp. 34–41, Mar. 2014.
[33] D. A. K. Pham and E. Gockenbach, "Analysis of physical transformer circuits for frequency response interpretation and mechanical failure diagnosis," *IEEE Trans. Dielectr. Electr. Insul.*, vol. 23, no. 3, pp. 1491–1499, Jun. 2016.
[34] B. A. Mork, F. Gonzalez, D. Ishchenko, D. L. Stuehm, and J. Mitra, "Hybrid transformer model for transient simulation—Part I: Development and parameters," *IEEE Trans. Power Deliv.*, vol. 22, no. 1, pp. 248–255, Jan. 2007.
[35] B. A. Mork, F. Gonzalez, D. Ishchenko, D. L. Stuehm, and J. Mitra, "Hybrid transformer model for transient simulation—Part II: Laboratory measurements and benchmarking," *IEEE Trans. Power Deliv.*, vol. 22, no. 1, pp. 256–262, Jan. 2007.
[36] S. Peng Ang, J. Li, Z. Wang, and P. Jarman, "FRA low frequency characteristic study using duality transformer core modeling," in *Proc. Int. Conf. Condition Monitor. Diagnosis*, 2008, pp. 889–893.
[37] W. Herrera, G. Aponte, J. Pleite, and C. Gonzalez-Garcia, "A novel methodology for transformer low-frequency model parameters identification," *Int. J. Electr. Power Energy Syst.*, vol. 53, pp. 643–648, Dec. 2013.
[38] W. Herrera Portilla, G. Aponte Mayor, J. Pleite Guerra, and C. Gonzalez-Garcia, "Detection of transformer faults using frequency-response traces in the low-frequency bandwidth," *IEEE Trans. Ind. Electron.*, vol. 61, no. 9, pp. 4971–4978, Sep. 2014.
[39] W. Herrera, G. Aponte, C. Gonzalez-Garcia, and J. Pleite, "Novel procedure for low frequency FRA traces interpretation," in *Proc. 20th Int. Conf. Electr. Mach.*, Sep. 2012, pp. 2344–2350.
[40] L. Satish and A. Saravanakumar, "Identification of terminal connection and system function for sensitive frequency response measurement on transformers," *IEEE Trans. Power Del.*, vol. 23, no. 2, pp. 742–750, Apr. 2008.
[41] J. Zhijian, Z. Minglin, and Z. Zishu, "Fault location of transformer winding deformation using frequency response analysis," in *Proc. Int. Symp. Electr. Insulating Mater. (ISEIM) Asian Conf. Electr. Insulating Diagnosis (ACEID) 33rd Symp. Electr. Electron. Insulating Mater. Appl. Syst.*, 2001, pp. 841–844.
[42] J. A. S. B. Jayasinghe, Z. D. Wang, P. N. Jarman, and A. W. Darwin, "Winding movement in power transformers: A comparison of FRA measurement connection methods," *IEEE Trans. Dielectr. Electr. Insul.*, vol. 13, no. 6, pp. 1342–1349, Dec. 2006.
[43] R. Khalili Senobari, J. Sadeh, and H. Borsi, "Frequency response analysis (FRA) of transformers as a tool for fault detection and location: A review," *Electric Power Syst. Res.*, vol. 155, pp. 172–183, Feb. 2018.
[44] *Measurement of Frequency Response*, document IEC 60076-18, vol. Ed.1, no. 18, 2012.
[45] CIGRE, "Mechanical condition assessment of transformer windings using frequency response analysis (FRA)," CIGRE, Paris, France, Tech. Broch. no. 342, 2008.
[46] *IEEE Guide for the Application and Interpretation of Frequency Response Analysis for Oil-Immersed Transformers*, IEEE Standard C57. 149, 2012.
[47] *Frequency Response Analysis on Winding Deformation of Power Transformers*, Chinese Standard DL/T911, 2004.
[48] *Interpretation of Sweep Frequency Response Analysis (SFRA) Measurement Results*, F. (OMICRON) Predl, Sydney, NSW, Australia, 2016.
[49] S. Tenbohlen and S. A. Ryder, "Making frequency response analysis measurements: A comparison of the swept frequency and low voltage impulse methods," in *Proc. 18th Int. Symp. High Voltage Eng.*, Delft, The Netherlands, 2003, pp. 25–29.
[50] A. Kraetge, M. Kruger, and P. Fong, "Frequency response analysis-status of the worldwide standardization activities," in *Proc. Int. Conf. Condition Monitor. Diagnosis*, 2008, pp. 651–654.
[51] T. Sano and K. Miyagi, "Influence factors on FRA waveforms," in *Proc. IEEE Int. Conf. Condition Monitor. Diagnosis*, Sep. 2012, pp. 601–604.
[52] Y. Liu, S. Ji, F. Yang, Y. Cui, L. Zhu, Z. Rao, C. Ke, and X. Yang, "A study of the sweep frequency impedance method and its application in the detection of internal winding short circuit faults in power transformers," *IEEE Trans. Dielectr. Electr. Insul.*, vol. 22, no. 4, pp. 2046–2056, Aug. 2015.
[53] J. Christian and K. Feser, "Procedures for detecting winding displacements in power transformers by the transfer function method," *IEEE Trans. Power Del.*, vol. 19, no. 1, pp. 214–220, Jan. 2004.
[54] M. H. Samimi, A. A. Shayegani Akmal, H. Mohseni, and S. Tenbohlen, "Detection of transformer mechanical deformations by comparing different FRA connections," *Int. J. Electr. Power Energy Syst.*, vol. 86, pp. 53–60, Mar. 2017.

[55] A. A. Pandya and B. R. Parekh, "Interpretation of sweep frequency response analysis (SFRA) traces for the open circuit and short circuit winding fault damages of the power transformer," *Int. J. Electr. Power Energy Syst.*, vol. 62, pp. 890–896, Nov. 2014.

[56] J. R. Secue and E. Mombello, "Sweep frequency response analysis (SFRA) for the assessment of winding displacements and deformation in power transformers," *Electric Power Syst. Res.*, vol. 78, no. 6, pp. 1119–1128, Jun. 2008, doi: 10.1016/j.epsr.2007.08.005.

[57] L. Satish and S. K. Sahoo, "Locating faults in a transformer winding: An experimental study," *Electric Power Syst. Res.*, vol. 79, no. 1, pp. 89–97, Jan. 2009.

[58] X. Lei, J. Li, Y. Wang, S. Mi, and C. Xiang, "Simulative and experimental investigation of transfer function of inter-turn faults in transformer windings," *Electric Power Syst. Res.*, vol. 107, pp. 1–8, Feb. 2014.

[59] B. Cheng, Z. Wang, and P. Crossley, "Using lumped element equivalent network model to derive analytical equations for interpretation of transformer frequency responses," *IEEE Access*, vol. 8, pp. 179486–179496, 2020, doi: 10.1109/ACCESS.2020.3027798.

[60] V. Behjat and M. Mahvi, "Statistical approach for interpretation of power transformers frequency response analysis results," *IET Sci., Meas. Technol.*, vol. 9, no. 3, pp. 367–375, May 2015.

[61] V. Behjat, A. Vahedi, A. Setayeshmehr, H. Borsi, and E. Gockenbach, "Sweep frequency response analysis for diagnosis of low level short circuit faults on the windings of power transformers: An experimental study," *Int. J. Electr. Power Energy Syst.*, vol. 42, no. 1, pp. 78–90, Nov. 2012.

[62] H. Firoozi and M. Shishehchian, "Frequency response analysis-condition assessment of power transformers using mathematical and statistical criteria," in *Proc. IEEE 9th Int. Conf. Properties Appl. Dielectric Mater.*, Jul. 2009, pp. 253–256.

[63] E. Rahimpour and D. Gorzin, "A new method for comparing the transfer function of transformers in order to detect the location and amount of winding faults," *Electr. Eng.*, vol. 88, no. 5, pp. 411–416, Jun. 2006.

[64] J.-W. Kim, B. Park, S. C. Jeong, S. W. Kim, and P. Park, "Fault diagnosis of a power transformer using an improved frequency-response analysis," *IEEE Trans. Power Del.*, vol. 20, no. 1, pp. 169–178, Jan. 2005.

[65] A. S. A. Razzaq, M. F. M. Yousof, S. M. Al-Ameri, M. A. Talib, and A. J. Mshkil, "Interpretation of inter-turn fault in transformer winding using turns ratio test and frequency response analysis," *Int. J. Electr. Electron. Eng. Telecommun.*, vol. 11, pp. 218–225, Jun. 2022.

[66] O. E. Gouda and S. H. El-Hoshy, "Diagnostic technique for analysing the internal faults within power transformers based on sweep frequency response using adjusted *R*-square methodology," *IET Sci. Meas. Technol.*, vol. 14, no. 10, pp. 1057–4068, 2020.

[67] M. Prameela and P. M. Nirgude, "Application of numerical techniques to FRA data for diagnosing integrity of transformer windings," in *Proc. Int. Conf. Condition Assessment Techn. Electr. Syst. (CATCON)*, Dec. 2015, pp. 87–92.

[68] P. Karimifard and G. B. Gharehpetian, "A new algorithm for localization of radial deformation and determination of deformation extent in transformer windings," *Electric Power Syst. Res.*, vol. 78, no. 10, pp. 1701–1711, Oct. 2008.

[69] E. Rahimpour, M. Jabbari, and S. Tenbohlen, "Mathematical comparison methods to assess transfer functions of transformers to detect different types of mechanical faults," *IEEE Trans. Power Del.*, vol. 25, no. 4, pp. 2544–2555, Oct. 2010.

[70] M. Khanali, A. Hayati-Soloot, H. K. Høidalen, and S. Jayaram, "Study on locating transformer internal faults using sweep frequency response analysis," *Electric Power Syst. Res.*, vol. 145, pp. 55–62, Apr. 2017.

[71] K. Ludwikowski, K. Siodla, and W. Ziomek, "Investigation of transformer model winding deformation using sweep frequency response analysis," *IEEE Trans. Dielectr. Electr. Insul.*, vol. 19, no. 6, pp. 1957–1961, Dec. 2012.

[72] K. Pourhossein, G. B. Gharehpetian, E. Rahimpour, and B. N. Araabi, "A probabilistic feature to determine type and extent of winding mechanical defects in power transformers," *Electric Power Syst. Res.*, vol. 82, no. 1, pp. 1–10, Jan. 2012.

[73] M. H. Samimi, S. Tenbohlen, A. A. S. Akmal, and H. Mohseni, "Using the complex values of the frequency response to improve power transformer diagnostics," in *Proc. 24th Iranian Conf. Electr. Eng. (ICEE)*, May 2016, pp. 1689–1693.

[74] M. H. Samimi, S. Tenbohlen, A. A. S. Akmal, and H. Mohseni, "Dismissing uncertainties in the FRA interpretation," *IEEE Trans. Power Del.*, vol. 33, no. 4, pp. 2041–2043, Aug. 2018.

[75] Y. Akhmetov, V. Nurmanova, M. Bagheri, A. Zollanvari, and G. B. Gharehpetian, "A new diagnostic technique for reliable decision-making on transformer FRA data in interturn short-circuit condition," *IEEE Trans. Ind. Informat.*, vol. 17, no. 5, pp. 3020–3031, May 2021, doi: 10.1109/TII.2020.3007607.

[76] V. Nurmanova, Y. Akhmetov, M. Bagheri, A. Zollanvari, B. T. Phung, and G. B. Gharehpetian, "Confidence level estimation for advanced decision-making in transformer short-circuit fault diagnosis," *IEEE Trans. Ind. Appl.*, vol. 58, no. 1, pp. 233–241, Jan. 2022.

[77] M. Tahir, S. Tenbholen, and S. Miyazaki, "Analysis of statistical methods for assessment of power transformer frequency response measurements," *IEEE Trans. Power Del.*, vol. 36, no. 2, pp. 618–626, Apr. 2021, doi: 10.1109/TPWRD.2020.2987205.

[78] S. M. A. N. Al-Ameri, M. S. Kamarudin, M. F. M. Yousof, A. A. Salem, F. A. Banakhr, M. I. Mosaad, and A. Abu-Siada, "Understanding the influence of power transformer faults on the frequency response signature using simulation analysis and statistical indicators," *IEEE Access*, vol. 9, pp. 70935–70947, 2021, doi: 10.1109/ACCESS.2021.3076984.

[79] Y. Akhmetov, V. Nurmanova, M. Bagheri, A. Zollanvari, and G. B. Gharehpetian, "A bootstrapping solution for effective interpretation of transformer winding frequency response," *IEEE Trans. Instrum. Meas.*, vol. 71, pp. 1–11, 2022.

[80] B. A. Thango, A. F. Nnachi, G. A. Dlamini, and P. N. Bokoro, "A novel approach to assess power transformer winding conditions using regression analysis and frequency response measurements," *Energies*, vol. 15, no. 7, p. 2335, Mar. 2022.

[81] M. Bigdeli and A. Abu-Siada, "Clustering of transformer condition using frequency response analysis based on k-means and GOA," *Electric Power Syst. Res.*, vol. 202, Jan. 2022, Art. no. 107619.

[82] H. Tarimoradi, H. Karami, G. B. Gharehpetian, and S. Tenbohlen, "Sensitivity analysis of different components of transfer function for detection and classification of type, location and extent of transformer faults," *Measurement*, vol. 187, Jan. 2022, Art. no. 110292.

[83] P. Karimifard, G. B. Gharehpetian, and S. Tenbohlen, "Localization of winding radial deformation and determination of deformation extent using vector fitting-based estimated transfer function," *Eur. Trans. Electr. Power*, vol. 19, no. 5, pp. 749–762, Jul. 2009.

[84] M. Bigdeli, M. Vakilian, and E. Rahimpour, "A new method for detection and evaluation of winding mechanical faults in transformer through transfer function measurements," *Adv. Electr. Comput. Eng.*, vol. 11, no. 2, pp. 23–30, 2011.

[85] M. F. M. Yousof, C. Ekanayake, and T. K. Saha, "Frequency response analysis to investigate deformation of transformer winding," *IEEE Trans. Dielectr. Electr. Insul.*, vol. 22, no. 4, pp. 2359–2367, Aug. 2015.

[86] M. F. M. Yousof, C. Ekanayake, and T. K. Saha, "Locating inter-disc faults in transformer winding using frequency response analysis," in *Proc. Australas. Universities Power Eng. Conf. (AUPEC)*, Sep. 2013, pp. 1–6.

[87] J. C. Gonzales and E. E. Mombello, "Diagnosis of power transformers through frequency response analysis by poles and zeros shifts identification," in *Proc. 6th IEEE/PES Transmiss. Distribution: Latin Amer. Conf. Exposit. (T&D-LA)*, Sep. 2012, pp. 1–8.

[88] A. J. Ghanizadeh and G. B. Gharehpetian, "ANN and cross-correlation based features for discrimination between electrical and mechanical defects and their localization in transformer winding," *IEEE Trans. Dielectr. Electr. Insul.*, vol. 21, no. 5, pp. 2374–2382, Oct. 2014.

[89] M. Bigdeli, M. Vakilian, and E. Rahimpour, "Transformer winding faults classification based on transfer function analysis by support vector machine," *IET Electr. Power Appl.*, vol. 6, no. 5, pp. 268–276, May 2012.

[90] H. Tarimoradi and G. B. Gharehpetian, "Novel calculation method of indices to improve classification of transformer winding fault type, location, and extent," *IEEE Trans. Ind. Informat.*, vol. 13, no. 4, pp. 1531–1540, Aug. 2017.

[91] A. Contin, G. Rabach, J. Borghetto, M. D. Nigris, R. Passaglia, and G. Rizzi, "Frequency-response analysis of power transformers by means of fuzzy tools," *IEEE Trans. Dielectr. Electr. Insul.*, vol. 18, no. 3, pp. 900–909, Jun. 2011.

[92] J. Liu, Z. Zhao, C. Tang, C. Yao, C. Li, and S. Islam, "Classifying transformer winding deformation fault types and degrees using FRA based on support vector machine," *IEEE Access*, vol. 7, pp. 112494–112504, 2019, doi: 10.1109/ACCESS.2019.2932497.

[93] V. Nurmanova, M. Bagheri, A. Zollanvari, K. Aliakhmet, Y. Akhmetov, and G. B. Gharehpetian, "A new transformer FRA measurement technique to reach smart interpretation for inter-disk faults," *IEEE Trans. Power Del.*, vol. 34, no. 4, pp. 1508–1519, Aug. 2019, doi: 10.1109/TPWRD.2019.2909144.

[94] X. Wu, Y. He, C. Wang, W. Wu, C. Wang, and J. Duan, "Hilbert ID considering multi-window feature extraction for transformer deep vision fault positioning," *IEEE Access*, vol. 8, pp. 91276–91286, 2020, doi: 10.1109/ACCESS.2020.2991844.

[95] M. Bigdeli, P. Siano, and H. H. Alhelou, "Intelligent classifiers in distinguishing transformer faults using frequency response analysis," *IEEE Access*, vol. 9, pp. 13981–13991, 2021, doi: 10.1109/ACCESS.2021.3052144.

[96] R. S. De Andrade Ferreira, P. Picher, H. Ezzaidi, and I. Fofana, "Frequency response analysis interpretation using numerical indices and machine learning: A case study based on a laboratory model," *IEEE Access*, vol. 9, pp. 67051–67063, 2021, doi: 10.1109/ACCESS.2021.3076154.

[97] R. Behkam, A. Moradzadeh, H. Karami, and M. S. Nadery, "Mechanical fault types detection in transformer windings using interpretation of frequency responses via multilayer perceptron," *J. Oper. Autom. Power Eng.*, vol. 11, no. 1, pp. 11–21, 2023.

[98] R. Behkam, H. Karami, M. S. Naderi, and G. B. Gharehpetian, "Generalized regression neural network application for fault type detection in distribution transformer windings considering statistical indices," *COMPEL Int. J. Comput. Math. Electr. Electron. Eng.*, vol. 41, no. 1, pp. 381–409, Jan. 2022.

[99] H. Ezziane, H. Houassine, S. Moulahoum, and M. S. Chaouche, "A novel method to identification type, location, and extent of transformer winding faults based on FRA and SMOTE-SVM," *Russian J. Nondestruct. Test.*, vol. 58, no. 5, pp. 391–404, May 2022.

[100] O. Elahi, R. Behkam, G. B. Gharehpetian, and M. N. Heris, "A new data mining application in smart monitoring systems using self organizing map neural network to distinguish disk space variations in distribution transformers," in *Proc. IEEE Electr. Power Energy Conf. (EPEC)*, Dec. 2022, pp. 248–254.

[101] O. Aljohani and A. Abu-Siada, "Application of DIP to detect power transformers axial displacement and disk space variation using FRA polar plot signature," *IEEE Trans. Ind. Informat.*, vol. 13, no. 4, pp. 1794–1805, Aug. 2017.

[102] O. Aljohani and A. Abu-Siada, "Application of digital image processing to detect short-circuit turns in power transformers using frequency response analysis," *IEEE Trans. Ind. Informat.*, vol. 12, no. 6, pp. 2062–2073, Dec. 2016.

[103] G. Ma, Y. Liu, Y. Li, X. Fan, C. Xu, and W. Qin, "Optical frequency-response analysis for power transformer," *IEEE Trans. Power Del.*, vol. 36, no. 3, pp. 1562–1570, Jun. 2021, doi: 10.1109/TPWRD.2020.3011422.

[104] J. C. Gonzales and E. E. Mombello, "Fault interpretation algorithm using frequency-response analysis of power transformers," *IEEE Trans. Power Del.*, vol. 31, no. 3, pp. 1034–1042, Jun. 2016.

[105] A. J. Ghanizadeh and G. B. Gharehpetian, "Application of characteristic impedance and wavelet coherence technique to discriminate mechanical defects of transformer winding," *Electric Power Compon. Syst.*, vol. 41, no. 9, pp. 868–878, Jul. 2013.

[106] E. Kornatowski and S. Banaszak, "Diagnostics of a transformer's active part with complementary FRA and VM measurements," *IEEE Trans. Power Del.*, vol. 29, no. 3, pp. 1398–1406, Jun. 2014.

[107] S. Banaszak and E. Kornatowski, "Evaluation of FRA and VM measurements complementarity in the field conditions," *IEEE Trans. Power Del.*, vol. 31, no. 5, pp. 2123–2130, Oct. 2016.

[108] Z. Wang, J. Li, and D. M. Sofian, "Interpretation of transformer FRA responses—Part I: Influence of winding structure," *IEEE Trans. Power Del.*, vol. 24, no. 2, pp. 703–710, Apr. 2009.

[109] M. Bagheri, B. T. Phung, and T. Blackburn, "Transformer frequency response analysis: Mathematical and practical approach to interpret mid-frequency oscillations," *IEEE Trans. Dielectr. Electr. Insul.*, vol. 20, no. 6, pp. 1962–1970, Dec. 2013.

[110] D. M. Sofian, Z. Wang, and J. Li, "Interpretation of transformer FRA responses—Part II: Influence of transformer structure," *IEEE Trans. Power Del.*, vol. 25, no. 4, pp. 2582–2589, Oct. 2010.

[111] N. Abeywickrama, Y. V. Serdyuk, and S. M. Gubanski, "Effect of core magnetization on frequency response analysis (FRA) of power transformers," *IEEE Trans. Power Del.*, vol. 23, no. 3, pp. 1432–1438, Jul. 2008.

[112] S. Zhang, C. Yao, X. Zhao, J. Li, X. Liu, L. Yu, J. Ma, and S. Dong, "Improved flux-controlled VFCV strategy for eliminating and measuring the residual flux of three-phase transformers," *IEEE Trans. Power Del.*, vol. 35, no. 3, pp. 1237–1248, Jun. 2020.

[113] M. F. M. Yousof, C. Ekanayake, and T. K. Saha, "An investigation on the influence of tap changer on frequency response analysis," in *Proc. IEEE 11th Int. Conf. Properties Appl. Dielectric Mater. (ICPADM)*, Jul. 2015, pp. 963–966.

[114] N. Hashemnia, A. Abu-Siada, and S. Islam, "Detection of power transformer bushing faults and oil degradation using frequency response analysis," *IEEE Trans. Dielectr. Electr. Insul.*, vol. 23, no. 1, pp. 222–229, Feb. 2016.

[115] O. Aljohani and A. Abu-siada, "Identification of the minimum detection of transformer bushing failure based on frequency response analysis (FRA)," in *Proc. IEEE 2nd Annu. Southern Power Electron. Conf. (SPEC)*, Dec. 2016, pp. 1–5.

[116] M. Bagheri, B. T. Phung, and T. Blackburn, "Influence of temperature and moisture content on frequency response analysis of transformer winding," *IEEE Trans. Dielectr. Electr. Insul.*, vol. 21, no. 3, pp. 1393–1404, Jun. 2014.

[117] M. Bagheri, B. T. Phung, and T. Blackburn, "Temperature influence on FRA spectrum of oil-filled and oil-free single-phase transformer," in *Proc. IEEE 11th Int. Conf. Properties Appl. Dielectric Mater. (ICPADM)*, Jul. 2015, pp. 955–958.

[118] A. A. Reykherdt and V. Davydov, "Case studies of factors influencing frequency response analysis measurements and power transformer diagnostics," *IEEE Elect. Insul. Mag.*, vol. 27, no. 1, pp. 22–30, Jan. 2011.

[119] M. Bagheri, B. T. Phung, T. Blackburn, and A. Naderian, "Influence of temperature on frequency response analysis of transformer winding," in *Proc. IEEE Electr. Insul. Conf. (EIC)*, Jun. 2013, pp. 40–44.

[120] M. Bagheri, B. T. Phung, and T. Blackburn, "Paper moisture variation vs. mechanical deformation impacts on transformer frequency response spectrum," in *Proc. Int. Symp. Electr. Insulating Mater.*, Jun. 2014, pp. 128–131.

[121] J. M. Guerrero, A. E. Castilla, J. A. S. Fernández, and C. A. Platero, "Transformer oil diagnosis based on a capacitive sensor frequency response analysis," *IEEE Access*, vol. 9, pp. 7576–7585, 2021, doi: 10.1109/ACCESS.2021.3049192.

[122] M. Bigdeli, "Hybrid K-means-PSO technique for transformer insulation moisture determination in the production stage based on frequency response analysis," *Iran. J. Electr. Electron. Eng.*, vol. 18, no. 1, p. 2072, 2022.

[123] J. C. Gonzales and E. E. Mombello, "Automatic detection of frequency ranges of power transformer transfer functions for evaluation by mathematical indicators," in *Proc. 6th IEEE/PES Transmiss. Distribution, Latin Amer. Conf. Exposit. (TD-LA)*, 2012, pp. 1–8.

[124] A. Abu-Siada, N. Hashemnia, S. Islam, and M. A. S. Masoum, "Understanding power transformer frequency response analysis signatures," *IEEE Elect. Insul. Mag.*, vol. 29, no. 3, pp. 48–56, May 2013.

[125] N. Hashemnia, A. Abu-Siada, M. A. S. Masoum, and S. M. Islam, "Characterization of transformer FRA signature under various winding faults," in *Proc. IEEE Int. Conf. Condition Monitor. Diagnosis*, Sep. 2012, pp. 446–449.

[126] A. Amini, N. Das, and S. Islam, "Impact of buckling deformation on the FRA signature of power transformer," in *Proc. Australas. Universities Power Eng. Conf. (AUPEC)*, Sep. 2013, pp. 1–4.

[127] Y. Li, G. Liu, L. Zhang, L. Zhang, and Z. Lin, "Transformer winding deformation diagnosis using middle band frequency response analysis," in *Proc. IEEE Int. Conf. Solid Dielectr.*, Jul. 2007, pp. 677–680.

[128] N. Hashemnia, A. Abu-Siada, and S. Islam, "Improved power transformer winding fault detection using FRA diagnostics—Part 1: Axial displacement simulation," *IEEE Trans. Dielectr. Electr. Insul.*, vol. 22, no. 1, pp. 556–563, Feb. 2015.

[129] N. Hashemnia, A. Abu-Siada, and S. Islam, "Impact of axial displacement on power transformer FRA signature," in *Proc. IEEE Power Energy Soc. Gen. Meeting*, Jul. 2013, pp. 1–4.

[130] J. A. S. B. Jayasinghe, Z. D. Wang, P. N. Jarman, and A. W. Darwin, "Investigations on sensitivity of FRA technique in diagnosis of transformer winding deformations," in *Proc. Conf. Rec. IEEE Int. Symp. Electr. Insul.*, 2004, pp. 496–499.

[131] M. A. Sathya, A. J. Thomas, and S. Usa, "Prediction of transformer winding displacement from frequency response characteristics," in *Proc. IEEE 1st Int. Conf. Condition Assessment Techn. Electr. Syst. (CATCON)*, Dec. 2013, pp. 303–307.

[132] N. Hashemnia, A. Abu-Siada, and S. Islam, "Improved power transformer winding fault detection using FRA diagnostics—Part 2: Radial deformation simulation," *IEEE Trans. Dielectr. Electr. Insul.*, vol. 22, no. 1, pp. 564–570, Feb. 2015.

[133] E. Gomez-Luna, G. A. Mayor, C. Gonzalez-Garcia, and J. P. Guerra, "Current status and future trends in frequency-response analysis with a transformer in service," *IEEE Trans. Power Del.*, vol. 28, no. 2, pp. 1024–1031, Apr. 2013.

[134] C. Gonzalez, J. Pleite, V. Valdivia, and J. Sanz, "An overview of the on line application of frequency response analysis (FRA)," in *Proc. IEEE Int. Symp. Ind. Electron.*, Jun. 2007, pp. 1294–1299.

[135] A. Vandermaar, "On-line frequency response analysis system," EPRI Project Manag. Tech., Washington, DC, USA, Tech. Rep. 1001942, 2001.

[136] N. Shanmugam, B. Madanmohan, and R. Rajamani, "Influence of the load on the impulse frequency response approach based diagnosis of transformer's inter-turn short-circuit," *IEEE Access*, vol. 8, pp. 39454–39463, 2020.

[137] N. Shanmugam, S. Gopal, B. Madanmohan, S. P. Balaji, and R. Rajamani, "Diagnosis of inter-turn shorts of loaded transformer under various load currents and power factors; impulse voltage-based frequency response approach," *IEEE Access*, vol. 9, pp. 40811–40822, 2021, doi: 10.1109/ACCESS.2021.3064347.

[138] R. Kumar, A. Vaijayanthi, R. Deshmukh, B. Vedik, and C. K. Shiva, "A condition monitoring and fault detection in the windings of power transformer using impulse frequency response analysis," *Int. J. Syst. Assurance Eng. Manag.*, vol. 13, pp. 1–13, Jan. 2022.

[139] S. Seifi, P. Werle, A. A. Shayegani Akmal, and H. Mohseni, "Sweep reflection coefficient method for localization of internal faults in transformer windings," *Int. J. Electr. Power Energy Syst.*, vol. 137, May 2022, Art. no. 107781.

[140] A. Abu-Siada and S. Islam, "A new approach to identify power transformer criticality and asset management decision based on dissolved gas-in-oil analysis," *IEEE Trans. Dielectr. Electr. Insul.*, vol. 19, no. 3, pp. 1007–1012, Jun. 2012.

[141] P. A. Venikar, M. S. Ballal, B. S. Umre, and H. M. Suryawanshi, "A novel offline to online approach to detect transformer interturn fault," *IEEE Trans. Power Del.*, vol. 31, no. 2, pp. 482–492, Apr. 2016.

[142] B. Garcia, J. C. Burgos, and A. Alonso, "Transformer tank vibration modeling as a method of detecting winding deformations—Part I: Theoretical foundation," *IEEE Trans. Power Del.*, vol. 21, no. 1, pp. 157–163, Jan. 2006.

[143] D. Zacharias and R. Gokaraju, "Prototype of a negative-sequence turn-to-turn fault detection scheme for transformers," *IEEE Trans. Power Del.*, vol. 31, no. 1, pp. 122–129, Feb. 2016.

[144] L. M. R. Oliveira and A. J. M. Cardoso, "A permeance-based transformer model and its application to winding interturn arcing fault studies," *IEEE Trans. Power Del.*, vol. 25, no. 3, pp. 1589–1598, Jul. 2010.

[145] A. S. Masoum, N. Hashemnia, A. Abu-Siada, M. A. S. Masoum, and S. M. Islam, "Online transformer internal fault detection based on instantaneous voltage and current measurements considering impact of harmonics," *IEEE Trans. Power Del.*, vol. 32, no. 2, pp. 587–598, Apr. 2017.

[146] S. C. Athikessavan, E. Jeyasankar, S. S. Manohar, and S. K. Panda, "Interturn fault detection of dry-type transformers using core-leakage fluxes," *IEEE Trans. Power Del.*, vol. 34, no. 4, pp. 1230–1241, Aug. 2019.

[147] X. Ouyang, Q. Zhou, H. Shang, Y. Zheng, S. Pan, and J. Luo, "Towards a comprehensive evaluation on the online methods for monitoring transformer turn-to-turn faults," *IEEE Trans. Ind. Electron.*, early access, Oct. 18, 2022, doi: 10.1109/TIE.2022.3213918.

[148] V. Behjat, A. Vahedi, A. Setayeshmehr, H. Borsi, and E. Gockenbach, "Diagnosing shorted turns on the windings of power transformers based upon online FRA using capacitive and inductive couplings," *IEEE Trans. Power Del.*, vol. 26, no. 4, pp. 2123–2133, Oct. 2011.

**SEYED EBRAHIM HOSSEINI KAKOLAKI** was born in Shahrekord, Iran, in 1992. He received the B.Sc. degree in electrical engineering from Yazd University, Yazd, Iran, in 2015, the M.Sc. degree from the Iran University of Science and Technology, Tehran, Iran, in 2018. Since 2018 until 2021, he worked as a Ph.D. student and since 2021, as a Research Assistant at the Ferdowsi University of Mashhad, Mashhad, Iran. His current research interests include power system protection, fault detection, and transient analysis in power systems.

**VAHID HAKIMIAN** was born in Tabas, Iran, in 1993. He received the B.Sc. degree in electrical engineering from the University of Tehran, Tehran, Iran, in 2015, and the M.Sc. degree from Tarbiat Modares University, Tehran, in 2018. He then joined a consulting company where he works as an Engineering Consultant in the electrical power industry of Iran and in the field of HV substation design. He has also worked as a Research Assistant at the Ferdowsi University of Mashhad. His current research interests include power system operation and planning, power system protection, and electrical power distribution systems.

**JAVAD SADEH** was born in Mashhad, Iran, in 1968. He received the B.Sc. and M.Sc. degrees (Hons.) in electrical engineering from the Ferdowsi University of Mashhad, Mashhad, in 1990 and 1994, respectively, and the Ph.D. degree in electrical engineering from the Sharif University of Technology, Tehran, Iran, in collaboration the the Electrical Engineering Laboratory, Instituto Politécnico Nacional de Grenoble (INPG), Grenoble, France, in 2001. He is currently a Professor with the Department of Electrical Engineering, Ferdowsi University of Mashhad. His research interests include power system protection, dynamics, operation as well as renewable energy technologies.

**ELYAS RAKHSHANI** (Senior Member, IEEE) received the B.Sc. degree in power systems, in 2004, the master's degree in control systems, in 2008, and the Ph.D. degree (cum laude) in electrical engineering from Universitat Politècnica de Catalunya (UPC), Barcelona, Spain, in 2016. He is currently a Senior Control and Power Systems Engineer, leading the Algorithm and Control Group, HESStec Company, Spain, with a focus on dynamic low-inertia grids, hybrid energy storage integration, Previous to that he worked with ABB power grids as a senior power system consultant focusing on different projects related to stability analysis of low-inertia systems with grid integration of renewables. While he was with the IEPG research center as a postdoctoral research engineer at the Delft University of Technology (TU Delft), Netherlands. He worked with the IEPG center working on European projects (H2020 European projects) related to grid code assessment, control and dynamic stability analysis of low-inertia power systems with a high share of wind power. His research interests include modern power system control, dynamic stability, hybrid energy storage integration, converter control applications in power systems, and HVdc control for grid applications, frequency control. In 2018, he received an Extraordinary Doctoral Award from the Permanent Committee of the UPC Doctoral School for the contribution on different methodology for emulating virtual inertia after the Ph.D. degree. He is a member of the editorial board of *Power and Energy Society* (PES) journals, such as IEEE Transactions on Power Systems, IEEE Power Engineering Letters, *IET Generation Transmission and Distribution*, *IET Renewable Power Generation*, and IEEE System Journal.